IFAC

INTERNATIONAL FEDERATION
OF AUTOMATIC CONTROL

WARSZAWA 1969

Guidance and Control in Space

Fourth Congress of the International Federation of Automatic Control
Warszawa 16–21 June 1969

TECHNICAL SESSION
49

Organized by
Naczelna Organizacja Techniczna w Polsce

INTERNATIONAL FEDERATION OF AUTOMATIC CONTROL

Guidance and Control in Space

TECHNICAL SESSION No 49

FOURTH CONGRESS OF THE INTERNATIONAL
FEDERATION OF AUTOMATIC CONTROL
WARSZAWA 16 – 21 JUNE 1969

Organized by
Naczelna Organizacja Techniczna w Polsce

Contents

Wydawnictwa Czasopism Technicznych NOT - Polska

Zakład Poligraficzny WCT NOT. Zam. 62/69.

ОБ УСЛОВИЯХ УПРАВЛЯЕМОСТИ В ОДНОЙ ЗАДАЧЕ СБЛИЖЕНИЯ

Бабаков Н.А., Ким Д.П.

Институт автоматики и телемеханики
Москва
С.С.С.Р.

I. Рассмотрим задачу преследования точкой А точки Б при следующих условиях. Преследуемая точка Б движется прямолинейно и равномерно. Преследующая точка А имеет постоянную по величине скорость. Управлениями точки А служат ограниченные по величине угловые скорости. Скорость V_A преследующей точки А меньше скорости $V_Б$ преследуемой точки Б ($V_A \leq V_Б$).

В силу последнего условия точка А не всегда (не при всех начальных условиях) может попасть или достигнуть в некоторую Е-окрестность точки Б. В связи с этим возникает задача определения условия, при выполнении которого точка А в процессе преследования может попасть в точку Б. Это условие, которое будем называть условием физической возможности преследования, или короче, условием управляемости, в пространстве начальных условий преследования, выделяет область управляемости. Поэтому рассматриваемую задачу можно еще формулировать как задачу определения области управляемости в пространстве начальных условий преследования и дальше для краткости ее будем называть задачей об управляемости.

Задача об управляемости в "двумерном" случае - в случае плоскостного преследования - была рассмотрена в [I] .

Здесь же эта задача рассматривается в случае пространственного преследования.

2. Постановка задачи. При соответствующем выборе системы отсчета - направление оси АУ совпадает с вектором $\vec{V}_Б$ скорости точки Б, начало координат совпадает с местонахождением точки А в начальный момент преследования (см. рисунок) - уравнения движения точек А и Б соответственно принимают вид:

$$(2.1)\quad \begin{cases} \dot{x}_A = V_A \cos x_5 \cos x_4 \\ \dot{y}_A = V_A \cos x_5 \sin x_4 \\ \dot{z}_A = V_A \sin x_5 \\ \dot{x}_4 = u_1 \\ \dot{x}_5 = u_2 \end{cases}$$

$$(2.2)\quad \dot{x}_Б = 0,\ \dot{y}_Б = V_Б,\ \dot{z}_Б = 0$$

Управления точки А подчиняются условию

$$(2.3)\quad \forall t \ |u_1| \le \omega_1,\ |u_2| \le \omega_2$$

В начальный момент преследования t_0

$$(2.4)\quad \begin{gathered} x_A(t_0) = y_A(t_0) = z_A(t_0) = 0 \\ x_4(t_0) = x_4^0,\ x_5(t_0) = x_5^0 \\ x_Б(t_0) = x_1^0,\ y_Б(t_0) = x_2^0,\ z_Б(t_0) = x_3^0 \end{gathered}$$

Введем обозначение

$$(2.5)\quad x_1 = x_Б - x_A,\ x_2 = y_Б - y_A,\ x_3 = z_Б - z_A$$

Тогда из уравнений (2.I) и (2.2) получим систему:

$$
\begin{aligned}
\dot{x}_1 &= -V_A \cos x_5 \cos x_4 \\
\dot{x}_2 &= V_Б - V_A \cos x_5 \sin x_4 \\
\dot{x}_3 &= -V_A \sin x_5 \\
\dot{x}_4 &= u_1 \\
\dot{x}_5 &= u_2
\end{aligned}
\qquad (2.6)
$$

которая описывает относительное движение точек А и Б и, следовательно, процесс преследования точкой А точки Б. Начальные условия преследования записываются в следующем виде (см (2.4)):

$$(2.7)\quad x_1(t_0)=x_1^0,\ x_2(t_0)=x_2^0,\ x_3(t_0)=x_3^0,\ x_4(t_0)=x_4^0,\ x_5(t_0)=x_5^0$$

Задача об управляемости формулируется следующим образом. В пространстве X^0 начальных условий $x^0=(x_1^0, x_2^0, x_3^0, x_4^0, x_5^0)$ $(x^0 \in X^0)$ найти область управляемости в случае преследования, процесс которого описывается системой (2.6) и соотношением (2.3) при условии

$$(2.8)\quad V_A \le V_Б$$

Следует заметить, что постановка рассматриваемой задачи и метод ее решения не претерпят существенных изменений, если I) снять условие равномерности движения точек А и Б и принять, что величины скоростей точек А и Б как-то меняются во времени, и 2) считать, что преследующая и преследуемая точки являются сложными динамическими системами и при выводе уравнений преследования будут учитываться уравнения, которыми эти системы описываются.

3. Рассмотрим сначала, как решается задача об управляемости в "двухмерном" случае, когда все время движение точек А и Б происходит в плоскости (y, z). Уравнения преследования для этого случая можно получить, если в (2.6) положить $x_1 \equiv 0$, $x_4 \equiv \pi/2$.

$$(3.1)\quad \begin{cases} \dot{x}_2 = V_B - V_A \cos x_5 \\ \dot{x}_3 = -V_A \sin x_5 \\ \dot{x}_5 = u_2 \end{cases}$$

Множество Ω_1 возможных значений для управления u_2 определяется неравенством $|u_2| \le \omega_2$.

Обозначим через t_1 момент времени, когда точка А в процессе преследования в первый раз пересекает траекторию точки Б:

$$(3.2)\quad x_3(t_1) = 0$$

и $x_3(t) \neq 0$ при всех $t \in (t_0, t_1)$. Величины t_1 и $x(t_1)$ зависят от начального условия $\tilde{x}^0 = (x_2^0, x_3^0, x_5^0)$ преследования и управления u_2 . Если состояние $\tilde{x}^0$ управляемо, то существует такое управление $u_2 \in \Omega_1$, при котором x_2 в момент времени t_1 меньше или равно нулю: $x_2(t_1) \le 0$. Действительно, если при всех допустимых управлениях $x_2(t_1) > 0$, то это означает, что каково бы ни было управление $u_2(t) \in \Omega_1$, точка А в момент t_1 будет на траектории точки Б сзади и в силу условия (2.8) она не может догнать точку Б.

Таким образом, необходимым условием управляемости состояния $\tilde{x}^0$ является условие

$$(3.3)\qquad \min_{u_2 \in \Omega_1} x_2(t_1, \tilde{x}^0) \le 0$$

В случае, когда множество Ω_1 совпадает со всей прямой ($\omega_2 = \infty$), условие (3.3) является также достаточным. Если же множество Ω_1 допустимых управлений ограничено, то возможны такие начальные состояния $\tilde{x}^0$, при которых точка А, каково бы ни было управление $u_2 \in \Omega_1$, пересечет траекторию точки Б в первый раз спереди: $x_2(t_1) < 0$, а во второй раз – сзади точки Б : $x_2(t_2) > 0$, t_2 – момент времени, когда точка А пересекает траекторию цели во второй раз. В этом случае, несмотря на выполнение условия (3.3) достижение точкой А точки Б невозможно. Справедливо следующее предложение. Для того, чтобы состояние $\tilde{x}^0$ было управляемо, необходимо и достаточно, чтобы выполнялось условие (3.3) и хотя бы одно из условий:

$$(3.4)\qquad \max_{u_2 \in \Omega_1} x_2(t_1, \tilde{x}^0) \ge 0$$

$$(3.5)\qquad \min_{u_2 \in \Omega_1} x_2(t_2, \tilde{x}^0) \le 0$$

Необходимость. Необходимость условия (3.3) была показана. Необходимость выполнения хотя бы одного из неравенств (3.4) и (3.5) следует из того, что если ни одно из этих неравенств не выполняется, то точка А при выполнении условия (3.3) при любом $u_2 \in \Omega_1$, в момент $t = t_1$ будет впереди, а в момент $t = t_2$ – сзади точки Б. Но тогда, как мы уже отмечали, состояние $\tilde{x}^0$ неуправляемо.

Достаточность. Выполнение условия (3.3) означает существование для данного состояния $\tilde{x}^0$ управления, при котором точка А в момент t_1 пересечёт траекторию точки Б

сзади. Ясно, что при одновременном выполнении обоих этих условий должно существовать управление, при котором в момент t_1 точка А попадает в точку Б: $x_2(t_1) = 0$. Иначе говоря, в этом случае состояние $\tilde{x}^0$ управляемо. Управляемость состояния $\tilde{x}^0$ при выполнении условий (3.3) и (3.5) видно из следующих рассуждений. В этом случае точка А какой-то отрезок времени, принадлежащий интервалу (t_1, t_2), удаляется от траектории точки Б. Поэтому, варьируя это время соответствующим выбором управления, можно добиться, чтобы в момент $t = t_2$ наступило попадание. Наше утверждение полностью доказано.

Таким образом, решение задачи об управляемости в случае плоскостного преследования свелось к определению минимума и максимума функционала $x_2(t_1, \tilde{x}^0)$ и минимума функционала $x_2(t_2, \tilde{x}^0)$. Но чтобы найти минимум (максимум) функционала $x_2(t_1, \tilde{x}^0)$, нужно решить вариационную задачу майера, формулировку которой не трудно привести [1]. Для того, чтобы найти минимум функционала $x_2(t_2, \tilde{x}^0)$, нужно решить трехточечную вариационную задачу, в которой значение функции $\tilde{x}(t) = \{x_2(t), x_3(t), x_5(t)\}$ задается при трех значениях времени: t_0, t_1 и t_2. Метод решения многоточечной и, в частности трехточечной вариационной задачи рассмотрен, например, [2].

4.Перейдем теперь к общему случаю пространственного преследования. Необходимое и достаточное условие в этом случае уже нельзя формулировать так, как это было сделано выше. Например, из одновременного выполнения условий

$$\min_{u \in \Omega} x_2(t_1, x^0) < 0 \quad \text{и} \quad \max_{u \in \Omega} x_2(t_1, x_0) > 0$$

еще не следует управляемость состояния x°. Здесь $x^\circ = (x_1^\circ, x_2^\circ, x_3^\circ, x_4^\circ, x_5^\circ)$ - начальное условие преследования, t_1 как и в п.3, обозначает момент времени, когда точка А в первый раз в процессе преследования пересекает траекторию точки Б:

(4.I) $\quad x_1(t_1) = 0, \; x_3(t_1) = 0$

и хотя бы одно из этих равенств не выполняется при любых $t \in (t_0, t_1)$.

Но точно так же, как было сделано в п.3, можно показать, что необходимым условием управляемости состояния x° является выполнение неравенства

(4.2) $\quad \min\limits_{u \in \mathcal{U}} x_2(t_1, x^\circ) < 0$

Вариационную задачу, которую необходимо решить, чтобы найти минимум функционала $x_2(t_1, x^\circ)$, можно сформулировать следующим образом. Среди непрерывных и кусочно-дифференцируемых функций $x(t) = \{x_1(t), \dots, x_5(t)\}$, удовлетворяющих в интервале (t_0, t_1) системе уравнений (2.6), а на концах - условиям (2.7) и (4.I) и среди кусочно-непрерывных управлений $u(t) \in \mathcal{U}$, найти такие $x(t)$ и $u(t)$, при которых функционал

(4.2) $\quad S = x_2(t_1, x^\circ)$

принимает минимальное значение.

Будем решать эту задачу, пользуясь принципом максимума Л.С. Понтрягина.

Составим функцию Гамильтона

$$(4.3)\quad H = -\psi_1 V_A \cos x_5 \cos x_4 + \psi_2 (V_B - V_A \cos x_5 \sin x_4) - \psi_3 V_A \sin x_5 + \psi_4 u_1 + \psi_5 u_2$$

Выпишем "сопряженные" уравнения:

$$\dot\psi_1 = \dot\psi_2 = \dot\psi_3 = 0$$

$$(4.4)\quad \dot\psi_4 = -\psi_1 V_A \cos x_5 \sin x_4 + \psi_2 \cos x_5 \cos x_4 \cdot V_A$$

$$\dot\psi_5 = -\psi_1 V_A \sin x_5 \cos x_4 - \psi_2 V_A \sin x_4 \sin x_4 + \psi_3 V_A \cos x_5$$

В конечный момент времени t_1 переменные ψ_2, ψ_4, ψ_5 и функция H должны удовлетворять условиям [3],

$$(4.5)\quad \psi_2(t_1) = -1,\ \psi_4(t_1) = \psi_5(t_1) = 0$$

$$(4.6)\quad H(t_1) = [-\psi_1 V_A \cos x_5 \cos x_4 - V_B + V_A \cos x_5 \sin x_4 - \psi_3 V_A \sin x_5]_{t=t_1} = 0.$$

Из (4.4) и (4.5) имеем

$$(4.7)\quad \psi_1 = C_1,\ \psi_2 = C_2,\ \psi_3 = C_3$$

$$\dot\psi_4 = -C_1 V_A \cos x_5 \sin x_4 - V_A \cos x_5 \cos x_4$$

$$\dot\psi_5 = -C_1 V_A \sin x_5 \cos x_4 + V_A \sin x_5 \sin x_4 + C_3 V_A \cos x_5$$

Так как функция H не зависит явно от времени, то она постоянна и в силу (4.6) равна нулю:

$$(4.8)\quad -C_1 V_A \cos x_5 \cos x_4 - V_B + V_A \cos x_5 \sin x_4 - C_3 V_A \sin x_5 + \psi_4 u_1 + \psi_5 u_2 = 0$$

Из принципа максимума для оптимального управления при $\psi_4 \neq 0$ и $\psi_5 \neq 0$ имеем:

$$(4.9)\quad u_1 = \omega_1 \operatorname{sign} \psi_4,\ u_2 = \omega_2 \operatorname{sign} \psi_5$$

При $\psi_4 = 0$ и $\psi_5 = 0$ функция H не зависит явно от управления $u = (u_1, u_2)$ и принцип максимума не позволяет получить выражение для оптимального управления. Поэтому в

этом случае мы будем исходить из других соображений.

Пусть $\psi_4 = 0$ на некотором интервале. Тогда на этом интервале, исключая, быть может, концов этого интервала, равна нулю и производная функции ψ_4 : $\dot{\psi}_4 = 0$. Подставив в это равенство вместо $\dot{\psi}$ ее выражение из (4.4), получим уравнение

(4.10) $$\cos x_5 (c_1 \sin x_4 + \cos x_4) = 0$$

Используя геометрические построения и результаты, полученные в [I], можно показать, что равенство $\cos x_5 = 0$ на некотором невырожденном интервале при оптимальном управлении исключено. Поэтому из (4.10) следует равенство

$$c_1 \sin x_4 + \cos x_4 = 0,$$

откуда не трудно получить для x_4 выражение

(4.11) $$x_4 = k\pi - arc \sin \frac{1}{\sqrt{1+c_1^2}}$$

Таким образом, если функция ψ_4 тождественно равна нулю на некотором интервале, то на этом интервале, исключая, быть может, его граничных точек, параметр u_1, оптимального управления выражается равенством

(4.12) $$\tilde{u}_1 = \dot{x}_4 = 0$$

Предположим, что функция ψ_4 на интервале $[t_0, t_1]$ обращается в нуль в конечном числе изолированных

точек [x]. Тогда, так как допустимое управление предполагается кусочно-непрерывным и содержит конечное число точек разрыва, множество изолированных и граничных точек интервала, где функция ψ_4 обращается в нуль, будет конечным. Поэтому в этих точках можно, не нарушая условия оптимальности, значение параметра $\tilde{u}_1$ оптимального управления, положить равным нулю. Тогда для $\tilde{u}_1$ на всем интервале $[t_0, t_1]$ имеем:

$$\tilde{u}_1 = \omega_1 \operatorname{sign} \psi_4(t) \qquad (4.13)$$

где

$$\operatorname{sign} \psi_4(t) = \begin{cases} 1, & \psi_4(t) > 0 \\ 0, & \psi_4(t) = 0 \\ -1, & \psi_4(t) < 0 \end{cases}$$

Пусть теперь обращается в нуль на некотором интервале функция ψ_5. Тогда на этом интервале, исключая, быть может, его граничных точек, обращается в нуль производная $\dot{\psi}_5$:

$$-c_1 \sin x_5 \cos x_4 + \sin x_5 \sin x_4 + c_3 \cos x_5 = 0 \qquad (4.14)$$

Продифференцировав последнее тождество, после несложных преобразований, получим

$$\tilde{u}_2 = \frac{(c_1 \sin x_4 + \cos x_4)\,\tilde{u}_1}{(c_1 \cos x_4 - \sin x_4)\operatorname{ctg} x_5 + c_3} \qquad (4.15)$$

где $\tilde{u}_1$ – параметр оптимального управления, определяемый равенством (4.13). Формула (4.15), вообще говоря,

---

[x] Можно допустить, что изолированных точек, в которых функция ψ_4 обращается в нуль, бесконечное множество. Важно, чтобы мера этого множества была равна нулю.

справедлива в тех точках интервала, где $\dot{\psi}_5 = 0$, в которых функции x_4 и x_5 дифференцируемы. Но так как точек, в которых функции x_4 и x_5 недифференцируемы, конечное множество , не нарушая общности, можем считать, что формула (4.I5) справедлива на всем интервале, в котором $\dot{\psi}_5 \equiv 0$. Так же, как и выше, в изолированных и граничных точках интервала, где $\psi_5 = 0$, положим $\tilde{u}_2 = 0$. Тогда параметр $\tilde{u}_2$ оптимального управления в невырожденных интервалах, в которых производная $\dot{\psi}_5$ тождественно равна нулю, определяется формулой (4.I5), а в остальных точках интервала $[t_0, t_1]$ - формулой (4.9).

Итак, оптимальное управление $\tilde{u}(t) = \{\tilde{u}_1(t), \tilde{u}_2(t)\}$ найдено. Теперь, чтобы найти необходимое условие управляемости, нужно при $u = \tilde{u}(t)$ решить систему уравнений (2.6) и (4.4) при граничных условиях (2.7), (4.I), (4.5) и (4.6).

Литература

I. Бабаков Н.А., Ким Д.П., Об области управляемости и оптимальных траекториях сближения двух космических аппаратов. Доклад на симпозиуме ИФАК по автоматическому управлению в космосе, воде и под землей. Вена, I967.

2. Троицкий В.А., Вариационные методы решения задач оптимизации процессов управления. Труды Всесоюзного совещания по автоматике. Оптимальные системы. Статистические методы, " Наука", I967 г.

3. Розоноэр Л.И., Принцип максимума Л.С. Понтрягина в теории оптимальных систем. I,П. Автоматика и телемеханика, I959, т.XX, №№ I0, II.

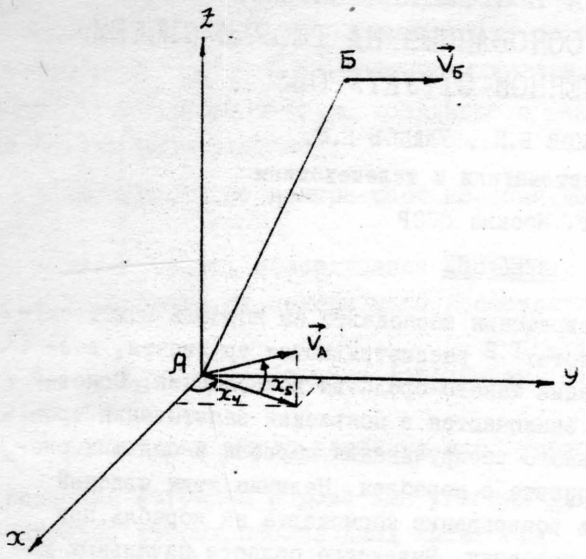

Рисунок.

$A(x_A, y_A, z_A)$ – координаты преследующей точки А ;

$Б(x_б, y_б, z_б)$ – координаты преследуемой точки Б ;

χ_y – угол между осью Ax и проекцией вектора $\vec{V}_A$ скорости точки А на плоскость (x, y);

χ_s – угол между плоскостью (x, y) и вектором скорости $\vec{V}_A$.

ДИНАМИКА ПЕРЕМЕЩЕНИЯ КОСМОНАВТА К КОРАБЛЮ С ПОМОЩЬЮ ТРОСА И ПРИНЦИП СИНТЕЗА УПРАВЛЕНИЯ КОРАБЛЕМ, ОСНОВАННЫЙ НА ТЕОРИИ СИСТЕМ С ПЕРЕМЕННОЙ СТРУКТУРОЙ

СОШНИКОВ В.Н., УЛАНОВ Г.М.
Институт автоматики и телемеханики
г. Москва СССР

ВВЕДЕНИЕ

Одним из средств возвращения космонавта на корабль может служить гибкий трос. В работах[1,2] рассматриваются трудности, возникающие при использовании такого средства возвращения. Основные из этих трудностей заключаются в появлении заматывания троса на корабль значительного раскручивания корабля и больших скоростей соударения космонавта с кораблем. Наличие этих явлений не позволяет обеспечить возвращение космонавта на корабль при произвольных начальных условиях. Выделение области начальных условий, при которых обеспечивается процесс возвращения с заданными ограничениями, составляет одну из задач работы. Решение этой задачи позволяет оценить практическую пригодность неуправляемой тросовой системы. Второй задачей работы является определение перспективного в данном случае метода синтеза углового управления кораблем, которое позволило бы устранить те свойства тросовой системы возвращения, которые затрудняют ее практическое использование. Указанные задачи решаются в случае плоского движения системы при постоянной скорости сматывания троса.

УРАВНЕНИЕ ДВИЖЕНИЯ СИСТЕМЫ

Математическая модель, принятая в работе, строится при следующих предположениях:

I. Корабль и космонавт - твердые тела.

2. Трос - нестационарная связь, изменяющаяся по линейному закону.

3. Внешние возмущения, в том, числе и от градиента гравитационного поля отсутствуют.

При этих предположениях уравнения движения центра масс и угловых движений системы независимы.

Динамическая модель углового движения и интересующие нас обобщенные координаты изображены на рис. I.

На рис. I обозначено:

I и 3 – корабль и космонавт с массами m_1 и m_3 и моментами инерции J_1 и J_3, относительно осей, проходящих через их центры масс O_1 и O_3, и перпендикулярных плоскости рисунка.

$X'O'Y'$ – инерциальная система координат с центром, расположенным в центре масс системы.

r_1 – расстояние от центра масс корабля до точки выхода троса.

r_2 – длина троса, изменяющаяся по закону: $r_2 = r_{20} + \dot{r}_{20} t$

r_3 – расстояние от центра масс космонавта до точки крепления троса.

φ_1, φ_2, φ_3, – обобщенные координаты, отсчитываемые относительно $X'O'Y'$

ℓ_t – расстояние между центрами масс корабля и космонавта.

Уравнения Лагранжа II рода для угловых движений, разрешенные относительно вторых производных имеют вид:

$$\ddot{\varphi}_1 = -\frac{F_2 r_1 \sin(\varphi_1-\varphi_2)}{J_1}$$

$$\ddot{\varphi}_2 = \frac{1}{r_2}\left[\frac{F_2 r_1^2 \cos(\varphi_1-\varphi_2)\sin(\varphi_1-\varphi_2)}{J_1} - \frac{F_2 r_3^2 \cos(\varphi_2-\varphi_3)\sin(\varphi_2-\varphi_3)}{J_3} - 2\dot{r}_{20}\dot{\varphi}_2 + r_1 \sin(\varphi_1-\varphi_2)\dot{\varphi}_1^2 + r_3 \sin(\varphi_2-\varphi_3)\dot{\varphi}_3^2\right] \qquad (I)$$

$$\ddot{\varphi}_3 = \frac{F_2 r_3 \sin(\varphi_2-\varphi_3)}{J_3}$$

где F_2 – сила натяжения троса, выражаемая формулой:

$$F_2 = \frac{K\left[r_1\cos(\varphi_1-\varphi_2)\dot{\varphi}_1^2 + r_2\dot{\varphi}_2^2 + r_3\cos(\varphi_2-\varphi_3)\dot{\varphi}_3^2\right]}{1 + \frac{K r_1^2 \sin^2(\varphi_1-\varphi_2)}{J_1} + \frac{K r_3^2 \sin^2(\varphi_2-\varphi_3)}{J_3}}; \quad K = \frac{m_1 m_3}{m_1+m_3} \qquad (2)$$

Система уравнений (I) допускает понижение порядка на две единицы, поскольку обобщенная координата φ_2 является циклической (или игнорируемой).

Процедуру понижения порядка удобно выполнить, вводя переменные Рауса[3], например, следующим образом: $t, \alpha_1, \alpha_2, \varphi_1, \dot{\alpha}_1, \dot{\alpha}_2, \rho_1$

где: $\rho_1 = \frac{\partial L}{\partial \dot{\varphi}_2}$ $\alpha_1 = \varphi_1 - \varphi_2$ $\alpha_2 = \varphi_3 - \varphi_2$ (3)

С помощью функции Рауса $R(t, \alpha_1, \alpha_2, \varphi_1, \dot{\alpha}_1, \dot{\alpha}_2, \rho_1)$, которая в нашем случае не зависит от φ_1, система (I) может быть заменена эквивалентной системой (4):

$$\begin{aligned}
&\frac{d}{dt}\left(\frac{\partial R}{\partial \dot{\alpha}_1}\right) - \frac{\partial R}{\partial \alpha_1} = 0\\
&\frac{d}{dt}\left(\frac{\partial R}{\partial \dot{\alpha}_2}\right) - \frac{\partial R}{\partial \alpha_2} = 0\\
&\frac{d\varphi_1}{dt} = \frac{\partial R}{\partial \rho_1}\\
&\frac{d\rho_1}{dt} = -\frac{\partial R}{\partial \varphi_1}
\end{aligned} \qquad (4)$$

Поскольку функция Рауса не зависит от φ_1, то $\rho_1 = \rho_{10}$, и за-

дача интегрирования системы (4) сводится к интегрированию двух первых уравнений. В виде, разрешенном относительно вторых производных эти два уравнения записываются следующим образом:

$$\ddot{\alpha}_1 = \bar{c}_{11} f_{11} + c_{12}\dot{\alpha}_1^2 + c_{13}\dot{\alpha}_2^2 + c_{14}\dot{\alpha}_1\dot{\alpha}_2 + c_{15}\dot{\alpha}_1 + c_{16}\dot{\alpha}_2$$
$$\ddot{\alpha}_2 = \bar{c}'_{11} f'_{11} + c'_{12}\dot{\alpha}_1^2 + c'_{13}\dot{\alpha}_2^2 + c'_{14}\dot{\alpha}_1\dot{\alpha}_2 + c'_{15}\dot{\alpha}_1 + c'_{16}\dot{\alpha}_2 \qquad (5)$$

где $\bar{c}_{11}, \bar{c}'_{11}$ – функции α_1 и α_2

$c_{ik}, c'_{ik}, f_{11}, f'_{11}$ – функции α_1, α_2 и t.

После интегрирования уравнений относительного движения (5) угловая скорость корабля и его угловое положение относительно инерциального пространства определяются формулами (6) и (7):

$$\dot{\varphi}_1 = \frac{\rho_{10} + \dot{\alpha}_1\left[\kappa(r_3^2 + r_2 b_2 + r_2^2 + 2b_2 r_2 + b_1 b_2 + a_1 a_2) + J_3\right] - \dot{\alpha}_2\left[\kappa(r_3^2 + b_2 r_2 + b_1 b_2 + a_1 a_2) + J_3\right] + \kappa(a_1 + a_2)\dot{r}_{20}}{J_1 + J_3 + \kappa l_c^2} \qquad (6)$$

$$\varphi_1 = \int_0^t \dot{\varphi}_1(t)\,dt + \varphi_{10} \qquad (7)$$

где $a_1 = r_1 \sin\alpha_1 \quad a_2 = r_3 \sin\alpha_2 \quad b_1 = r_1 \cos\alpha_1 \quad b_2 = r_3 \cos\alpha_2$

$$l_c^2 = r_1^2 + r_2^2 + r_3^2 + 2b_1 r_2 + 2b_1 b_2 + 2a_1 a_2 + 2b_2 r_2 \qquad (8)$$

Величина ρ_1, как можно показать, представляет собой кинетический момент системы, а интеграл $\rho_1 = \rho_{10}$ системы (4) выражает закон сохранения кинетического момента. На основании изложенного можно сделать вывод о том, что уравнения относительного движения (5) совместно с формулами (6) и (7), дают полное описание движения исследуемой системы.

СТАЦИОНАРНЫЕ ДВИЖЕНИЯ СИСТЕМЫ

Положения равновесия системы (5), то есть такие точки α_1^*, α_2^*, для которых $\dot{\alpha}_1 \equiv \dot{\alpha}_2 \equiv \ddot{\alpha}_1 \equiv \ddot{\alpha}_2 \equiv 0$, могут быть определены как корни системы алгебраических уравнений (9):

$$\bar{c}_{11}(\alpha_1, \alpha_2) = 0$$
$$\bar{c}'_{11}(\alpha_1, \alpha_2) = 0 \qquad (9)$$

Решения системы (9) α_1^* и α_2^* могут быть вычислены с помощью величин a_1^* и a_2^*, которые определяются формулами (10)

$$a_1^* = r_1 \sin\alpha_1^* \qquad a_2^* = r_3 \sin\alpha_2^* \qquad (10)$$

Значения a_1^* и a_2^*, являющиеся решениями системы (9) определяются формулами:

$$a_{11}^* = -\frac{\rho_{10} + \kappa a_{21}^* \dot{r}_{20}}{\kappa \dot{r}_{20}} \qquad (11)$$

$$a_{12,13}^* = \frac{\rho_{10} J_1}{(J_1 + J_3)2\kappa\dot{r}_{20}} \pm \rho_{10}\sqrt{\left[\frac{J_1}{(J_1 + J_3)2\kappa\dot{r}_{20}}\right]^2 - \frac{2J_1^2}{\kappa(J_1 + J_3)\rho_{10}^2}}\,; \quad a_{22}^* = \frac{J_3}{J_1} a_{12}^*;\ a_{23}^* = \frac{J_3}{J_1} a_{13}^* \qquad (12)$$

где вторые индексы у a_1^* и a_2^* обозначают различные значения,

принимаемые решениями системы (9). Легко установить, что формуле (II) соответствует бесконечное множество стационарных движений системы, представляющих собой сближение по инерции со скоростью $\dot{r}_{20}$ невращающихся корабля и космонавта, имеющих относительно троса неизменное положение, при нулевой силе натяжения троса. Два стационарных движения, соответствующие формулам (I2), представляют собой некоторые движения, при которых имеет место раскручивание системы относительно инерциального пространства с возрастающей скоростью, тогда как взаимное положение корабля и космонавта относительно троса остается неизменным. Интересной особенностью равновесных состояний и стационарных движений системы является их зависимость не только от параметров системы, но и от начальных условий, которые и определяют величину кинетического момента ρ_{10}. Зависимость равновесных вещественных значений α_1^* от параметров системы и величины кинетического момента, а также знаки члена $C_{11} = \bar{C}_{11} f_{11}$ в правой части уравнений (5) удобно представить с помощью бифуркационной диаграммы (рис.2).

На рис. 2 обозначено:

$\overline{\overline{\text{I}}}$ и $\overline{\overline{\text{I}}}'$ – кривые, имеющие уравнение: $\rho_{10} = \pm\left[\kappa\dot{r}_{20}\frac{J_1+J_3}{J_1}a_1^* + \frac{2\dot{r}_{20}J_3}{a_1^*}\right]$

$\overline{\overline{\text{II}}}$ – кривые, заключенные между кривыми $\overline{\overline{\text{I}}}'$ и $\overline{\overline{\text{I}}}''$, имеющие уравнение $\rho_{10} = -\kappa(a_{11}^* + a_{21}^*)\dot{r}_{20}$ (I4) и при $a_{21}^* = +r_3$ и $a_{21}^* = -r_3$, превращающиеся соответственно в $\overline{\overline{\text{I}}}'$ и $\overline{\overline{\text{I}}}''$.

Функции α_1^* от ρ_{10} имеют вид $\overline{\overline{\text{I}}}$ или $\overline{\overline{\text{I}}}'$ в зависимости от того принимает ли величина:

$$a_{1m}^* = J_3\sqrt{\frac{2}{\kappa(J_1+J_3)}} \qquad (I5)$$

значения меньшие r_1 или большие r_1.

Значения угла α_1^*, отмеченные на рис. 2, определяются по формулам: $|\alpha_{12}^*| = \arcsin\frac{|a_{12}^*|}{r_1}$ $|\alpha_{12}^{*\prime}| = \pi - \arcsin\frac{|a_{12}^*|}{r_1}$ $|\alpha_{1m}^*| = \arcsin\frac{|a_{1m}^*|}{r_1}$

$|\alpha_{13}^*| = \arcsin\frac{|a_{13}^*|}{r_1}$ $|\alpha_{13}^{*\prime}| = \pi - \arcsin\frac{|a_{13}^*|}{r_1}$ $|\alpha_{1m}^{*\prime}| = \pi - \arcsin\frac{|a_{1m}^*|}{r_1}$ (I6)

Значения параметров ρ_{10}', $\bar{\rho}_{10}$ и ρ_{10}^{min}, при которых изменяется число положений равновесия, являются бифуркационными и определяются формулами:

$$\rho_{10}' = |\dot{r}_{20}|\left[\frac{2J_1}{r_1} + \frac{\kappa(J_1+J_3)r_1}{J_1}\right];\ \bar{\rho}_{10} = \kappa(r_1+r_3)|\dot{r}_{20}|;\ \rho_{10}^{min} = 2\sqrt{2}\,|\dot{r}_{20}|\sqrt{\kappa(J_1+J_3)} \qquad (I7)$$

Зависимость равновесных значений α_2^* от параметров системы и ρ_{10} имеет такой же вид, что и зависимость, приведенная на рис.2, с тем лишь отличием, что масштаб по оси α_2^* и формулы для кривых $\overline{\overline{\text{II}}}$ и $\overline{\overline{\text{II}}}'$ должны быть изменены в соответствии с формулой $a_1^* = \frac{J_1}{J_3}a_2^*$,

а бифуркационное значение параметра ρ'_{10} теперь определяется формулой:

$$\rho'_{10} = |\dot{\tau}_{20}| \left[\frac{2J_3}{\tau_3} + \frac{\kappa(J_1+J_3)}{J_3}\tau_3 \right] \qquad (18)$$

Поскольку значения α_1^* и α_2^*, отличающиеся на $2\kappa\pi$ ($\kappa=1,2\ldots$) соответствуют одной и той же конфигурации системы (подпространства $\alpha_1\dot{\alpha}_1$, $\alpha_2\dot{\alpha}_2$ - цилиндрические), то рассмотрение равновесных значений на интервале $(-\pi, \pi)$ исчерпывает все возможные состояния равновесия. Для бифуракционной диаграммы вида П характер основных типов относительного движения троса и корабля при $\rho_{10} > \rho'_{10}$ и $\rho_{10} < \rho'_{10}$ представлен на рис. 3.

ПРИБЛИЖЕННЫЕ УРАВНЕНИЯ, ОПИСЫВАЮЩИЕ ОТНОСИТЕЛЬНОЕ ДВИЖЕНИЕ КОРАБЛЯ И ТРОСА

Анализ стационарных движений был выполнен для произвольных геометрических и инерционных характеристик сближаемых объектов. При получении формул, описывающих относительное движение троса и корабля, используем то обстоятельство, что для системы возвращения космонавта имеют место следующие неравенства:

$$J_1 \gg J_3 \quad \tau_1 \gg \tau_3 \qquad (19)$$

В этом случае, как следует из формул для равновесных состояний α_1^* и бифуркационных значений параметров, структура фазового пространства модели системы, в которой космонавт представлен точечной массой, практически совпадает со структурой фазового подпространства $\alpha_2\dot{\alpha}_2$ рассматриваемой модели. Для этой упрощенной модели линеаризованные в окрестностых равновесных состояний α_{12}^*, $\alpha_{12}^{*\prime}$, α_{13}^*, $\alpha_{13}^{*\prime}$ уравнения относительного движения корабля и троса имеют вид:

$$\bar{\alpha}_1'' + A_1(\tau_2)\bar{\alpha}_1' + B_1(\tau_2)\bar{\alpha}_1 = 0 \qquad (20)$$

и линеаризованные в окрестностях равновесных состояний α_{11}^* и $\alpha_{11}^{*\prime}$ - вид:

$$\bar{\alpha}_1'' + A_1(\tau_2)\bar{\alpha}_1' + \bar{B}_1(\tau_2)\bar{\alpha}_1 = 0 \qquad (21)$$

где: $\bar{\alpha}_1 = \alpha_1 - \alpha_1^*$ и $\bar{\alpha}_1'$ обозначает дифференцирование по новой независимой переменной τ_2, линейно связанной с t. Величины $A_1(\tau_2)$, $B_1(\tau_2)$ и $\bar{B}_1(\tau_2)$ вычисляются для каждого из равновесных состояний по формулам:

$$A_1(\tau_2) = \frac{2(J_1 + \kappa\tau_1^2 + \kappa\ell_1^*\tau_2)}{\tau_2(J_1 + \kappa\ell_1^{*2})} \qquad (22)$$

$$B_1(\tau_2)=\frac{2b_1^*(2J_1-\kappa a_1^{*2})}{\tau_2(J_1+\kappa l_t^{*2})a_1^{*2}} \quad (23) \qquad \bar{B}_1(\tau_2)=-\frac{2\kappa b_1^*}{\tau_2(J_1+\kappa l_t^{*2})} \quad (24)$$

$$\text{где } l_t^{*2}=\tau_1^2+2b_1^*\tau_2+\tau_2^2 \quad (25), \qquad b_1^*=\tau_1\cos\alpha_1^* \quad (26)$$

и a_1^* вычисляется по одной из формул (10).

Уравнения (20) и (21) поддаются классификации, а именно, они представляют собой линейные дифференциальные уравнения класса Фукса[4] и обладают четырьмя особыми точками. Интегрирование таких уравнений представляет пока не решенную проблему. Рассмотрим свойства уравнений (20) и (21) и сравним их с соответствующими свойствами решений нелинейной системы (5) в окрестностях равновесных состояний. С помощью теорем, приведенных в[5], можно установить, что решения уравнений (20) и (21), соответствующих равновесным точкам α_{12}^{*I}, α_{13}^{*}, α_{14}^{*} не могут быть колеблющимися, тогда как решения уравнений (20) и (21), соответствующих равновесным точкам α_{12}^{*}, α_{13}^{*II} и α_{14}^{*II} на достаточно большом интервале изменения аргумента будут колебательными. В окрестности особой точки коэффициентов $\tau_2=0$ нули колебательных решений уравнений (20) и (21) не имеют точек накопления, а производная общего решения стремится с бесконечности, что можно установить интегрируя уравнения (20) и (21) в окрестности особой точки методом Фробениуса, как, например в[5] или [6]. С помощью моделирования нелинейной системы (5) можно установить совпадение свойств ее решений для относительного движения корабля и троса с установленными свойствами линейных уравнений (20) и (21).

С помощью теоремы Сонина-Пойа[5] можно установить, что последовательность экстремумов колебательных решений уравнений (20) и (21) является убывающей на интервале ($\tau_{20}, \tau_{21}^{\Phi_1}$) изменения τ_2 и возрастающей - на интервале ($\tau_{21}^{\Phi_1}, 0$). При условиях (19) величина $\tau_{21}^{\Phi_1}$ положительна и определяется формулой:

$$\tau_{21}^{\Phi_1}=\sqrt{\frac{J_1+\kappa\tau_1^2}{\kappa}} \quad (29)$$

На рис. 4 представлены точные решения I и II уравнений (20) и системы (5) для относительного движения корабля и троса в окрестности равновесной точки α_{12}^{*}. Из рис. 4 можно видеть, что решения линейного уравнения (20) обладают свойствами соответствующего решения нелинейной системы (5) в окрестности α_{12}^{*} и удовлетворительно совпадают количественно. Можно видеть также, что в

процессе возвращения решение существенно отклоняется от соответствующего равновесного состояния лишь в некоторой весьма малой окрестности точки $\tau_2 = 0$. Сказанное выше позволяет считать линейные уравнения (20) и (2I) приемлемыми для описания относительного движения троса и корабля.

АСИМПТОТИЧЕСКОЕ ПРЕДСТАВЛЕНИЕ РЕШЕНИЯ УРАВНЕНИЯ ОТНОСИТЕЛЬНОГО ДВИЖЕНИЯ ТРОСА И КОРАБЛЯ

Получим асимптотическое представление решения уравнений (20) и (2I) следуя[6]. С целью приведения уравнений (20) и (2I) к рассматриваемой в[6] форме введем большой параметр T изменением масштаба независимой переменной по формуле:

$$\tau = \frac{\tau_2}{T} \qquad (28)$$

Для упрощения выкладок приведем уравнения (20) и (2I) заменой неизвестной функции по формуле $\bar{\alpha}_1 = \exp\left(-\frac{1}{2}\int A_1(\tau_2)d\tau_2\right)\beta$ (29) к каноническому виду:

$$\beta'' + I(\tau_2)\beta = 0 \qquad (30)$$

где $I(\tau_2)$ может принимать значения $I_1(\tau_2) = B_1(\tau_2) - \frac{1}{4}A_1^2(\tau_2) - \frac{1}{2}A_1'(\tau_2)$ (3I) или $\bar{I}_1(\tau_2) = \bar{B}_1(\tau_2) - \frac{1}{4}A_1^2(\tau_2) - \frac{1}{2}A_1'(\tau_2)$ (32) в соответствии с коэффициентами уравнений (20) и (2I). Линейно независимые решения β_1 и β_2 отыскиваются в виде рядов по отрицательным степеням большого параметра, которые при несущественных в нашем случае ограничениях являются асимптотическими. Эти ряды даются формулами:

$$\beta_1 = e^{\int \lambda_1(\tau) T d\tau}\left[C_0(\tau) + C_1(\tau)\frac{1}{T} + \dots C_k(\tau)\frac{1}{T^k}\cdots\right]$$
$$\beta_2 = e^{\int \lambda_2(\tau) T d\tau}\left[\bar{C}_0(\tau) + \bar{C}_1(\tau)\frac{1}{T} + \dots \bar{C}_k(\tau)\frac{1}{T^k}\cdots\right] \qquad (33)$$

где $C_k(\tau), \bar{C}_k(\tau)$ неизвестные функции, определяемые из реккурентных соотношений:

$$2\lambda_1\dot{C}_0 + \dot{\lambda}_1 C_0 = 0$$
$$\ddot{C}_0 + 2\lambda_1\dot{C}_1 + \dot{\lambda}_1 C_1 = 0 \qquad (34)$$
$$\ddot{C}_k + 2\lambda_1\dot{C}_{k+1} + \dot{\lambda}_1 C_{k+1} = 0$$

$$2\lambda_2\dot{\bar{C}}_0 + \dot{\lambda}_2\bar{C}_0 = 0$$
$$\ddot{\bar{C}}_0 + 2\lambda_2\dot{\bar{C}}_1 + \dot{\lambda}_2\bar{C}_1 = 0 \qquad (35)$$
$$\ddot{\bar{C}}_k + 2\lambda_2\dot{\bar{C}}_{k+1} + \dot{\lambda}_2\bar{C}_{k+1} = 0$$

а $\lambda_{1,2} = \pm i\sqrt{I(\tau)}$ (36).

В рассматриваемом случае можно установить, что имеют место неравенства:

$$C_0(\tau) \gg \frac{C_1(\tau)}{\pi} \gg \dots \frac{C_k(\tau)}{\pi^k} \dots \quad \bar{C}_0(\tau) \gg \frac{\bar{C}_1(\tau)}{\pi} \gg \dots \frac{\bar{C}_k(\tau)}{\pi^k} \dots \quad (37)$$

за исключением, быть может, весьма малой окрестности точки $\tau_2 = 0$. Это обстоятельство позволяет ограничиться асимптотическим представлением решения уравнений (20) и (2I), которое имеет вид:

$$\alpha_1 = e^{-\frac{1}{2}\int A_1(\tau_2)d\tau_2} I^{-\frac{1}{4}}(\tau_2)\left[\alpha_1 e^{i\int\sqrt{I(\tau_2)}\,d\tau_2} + \alpha_2 e^{-i\int\sqrt{I(\tau_2)}\,d\tau_2}\right] \quad (38)$$

Можно установить, что решение, даваемое формулой (38), обладает свойствами, ранее установленными для решений уравнений (20) и (2I). О количественных оценках точности решения, даваемого формулой (38) можно судить по рис.5, на котором сплошной линией изображено асимптотическое представление решения и его огибающая, а пунктирной линией – точное решение линейного уравнения.

ОБЛАСТЬ ДОПУСТИМЫХ НАЧАЛЬНЫХ УСЛОВИЙ ОТНОСИТЕЛЬНОГО ДВИЖЕНИЯ ТРОСА И КОРАБЛЯ

С помощью формул (II), (I2), (I6) и (38) относительное движение троса и корабля задается как известная функция начальных условий движения, параметров системы и времени. Ограничения, наложенные на угол α_1 между тросом и кораблем, угловую скорость корабля в инерциальном пространстве $\dot{\varphi}_1$, силу натяжения троса F_2 и модуль вектора скорости соударения корабля и космонавта V, могут быть записаны в виде следующих неравенств (39):

$$\begin{aligned} &|\alpha_1(t)| \le \alpha_m \\ &|\dot{\varphi}_1(t)| \le \dot{\varphi}_m \\ &|F_2(t)| = F_2(t) \le F_m \\ &\sqrt{\left[\tau_2(T)\dot{\alpha}_1(T)\right]^2 + \dot{\tau}_{20}^2} \le V_m \end{aligned} \quad (39)$$

где T – момент причаливания, не совпадающий с моментом $\tau_2 = 0$ и выбираемый из конструктивных соображений. Неравенства (39) выделяют в пространстве начальных условий и параметров системы некоторую область с границей σ, которую мы будем называть областью допустимых условий – параметров системы. В работе определяется проекция границы этой области на плоскость начальных дальностей – тангенциальных скоростей космонавта,

с координатами r_{20} и $\psi_k = r_{20}\dot{\alpha}_{10}$. Результаты этого исследования представлены с помощью рис. 6 и рис. 7 для следующих параметров системы и принятых ограничений: $J_1 = 400\ кГ м сек^2$ $\dot{r}_{20} = 0{,}2\ \frac{м}{сек}$ $\kappa = 20\ \frac{кГ сек^2}{м}$ $\varphi_1 = \varphi_2$ $\alpha_m = \frac{\pi}{2}$ при различных фиксированных значениях F_m, $\dot{\varphi}_m$ и V_m. На рис. 6 обозначены: I – кривые, между которыми выполняется первое из неравенств (39) при $\dot{\varphi}_{10} = 0$, II – кривая, выше которой $|\alpha_1(t)| \le \alpha_m$ при $\dot{\varphi}_{10} = \dot{\varphi}_{20}$ $\dot{\varphi}_m, F_m$ – кривые, ниже которых выравняются второе и третье из неравенств (39) для соответствующих ограничений.

На рис. 6 одна из областей, удовлетворяющая первым трем из неравенств (39) заштрихована.

На рис. 7 обозначены:

$P_{10} < P_{10}^{min}$ – область, в которой кинетический момент системы меньше P_{10}^{min}

$V_m^{(1)}$ $V_m^{(1.5)}$ $V_m^{(2)}$ – кривые, левее которых выполняется последнее из неравенств (39); первые три кривые построены для случая $\dot{\varphi}_{10} = 0$, $\dot{\varphi}_{20} \neq 0$, а вторые три – для случая $\dot{\varphi}_{10} = \dot{\varphi}_{20}$.

Из рис. 6 и рис. 7 можно видеть, что для каждой начальной дальности космонавта его тангенциальные скорости из условия успешного возвращения должны быть ограничены сверху и снизу, что, по-видимому, исключает применение неуправляемой системы возвращения космонавта с помощью троса к космическому кораблю.

ПРИНЦИП СИНТЕЗА СИСТЕМЫ УПРАВЛЕНИЯ ОТНОСИТЕЛЬНЫМ ДВИЖЕНИЕМ ТРОСА И КОРАБЛЯ

В качестве возможной системы управления в работе рассматривается система углового управления кораблем с помощью двигателей, обладающих релейной характеристикой. Можно показать, что при условии (I9) относительное движение троса и корабля удовлетворительно описывается в случае принятого исполнительного устройства следующим уравнением:

$$\ddot{\alpha}_1 + \frac{J_1 + \kappa(r_1^2 + b_1 r_2)}{J_1 + \kappa l_t^2}\left[\frac{2\dot{r}_{20}}{r_2}\dot{\alpha}_1 + \frac{\kappa a_1 (b_1 + r_2)}{J_1 + \kappa a_1^2}\dot{\alpha}_1^2\right] + \frac{(P_{10} + \kappa a_1 \dot{r}_{20} - \int_0^t M \operatorname{sign} b_1\, dt)}{r_2 (J_1 + \kappa a_1^2)(J_1 + \kappa l_t^2)} \cdot$$

$$\cdot \left(P_{10} a_1 - \kappa a_1^2 \dot{r}_{20} - 2\dot{r}_{20} J_1\right) = \frac{M \operatorname{sign} b_1 (b_1 + r_2)}{r_2 (J_1 + \kappa a_1^2)} \qquad (40)$$

где $\ell_t^2 = r_1^2 + 2b_1r_2 + r_2^2$, M – управляющий момент, приложенный к кораблю, а σ_1 – сигнал управления.

После интегрирования уравнения (40) угловая скорость корабля и угол поворота корабля относительно инерциального пространства определяются формулами:

$$\dot{\varphi}_1 = \frac{P_{10} + \kappa a_1 \dot{r}_{20} - \kappa \dot{d}_1 r_2 (b_1 + r_2) + \int_0^t M \operatorname{sign} \sigma_1 dt}{J_1 + \kappa \ell_t^2}; \quad \varphi_1 = \int_0^t \dot{\varphi}(t) dt + \varphi_{10} \quad (41)$$

Значение параметра $M \operatorname{sign} \sigma_1$ входящего в уравнение (40), скачкообразно изменяется при переходе изображающей точкой в фазовом пространстве системы некоторой поверхности переключения $\sigma_1(d_1, \dot{d}_1) = 0$ (42).

Системы, описываемые такими уравнениями, и получившие название систем с переменной структурой, обладают рядом интересных особенностей, не присущих, вообще говоря, составляющим структурам[7], которые в нашем случае описываются нелинейными неавтономными уравнениями, зависящими от предистории движения. Важнейшей из этих особенностей является возможность обеспечения при некоторых условиях устойчивого движения системы вдоль поверхности переключения в, так называемом, "скользящем" режиме. В этом случае динамические свойства системы определяются в основном видом поверхности переключения и слабо зависят от параметров объекта. В рассматриваемой задаче обеспечение независимости управляемого движения от таких параметров как кинетический момент и длина троса позволяет получить систему, работающую в широком диапазоне начальных условий и не обладающую свойством значительного увеличения угловых скоростей в конце притягивания, приводящим к большим скоростям соударения. Сказанное выше позволяет сформулировать задачу синтеза системы управления относительным движением троса и корабля как задачу выбора поверхности переключения (42) таким образом, чтобы:

I. Поверхность (42) обладала бы областью "скольжения" Ω, такой, что в процессе движения по ней система приходила бы в заданную окрестность точки $d_1 = \dot{d}_1 = 0$ фазового пространства и оставалась в ней.

2. Фазовые траектории системы попадали в область Ω при произвольных начальных условиях движения.

3. Поверхность Ω соответствовала бы условиям качества.

В работе рассматривается частный случай проблемы, когда поверхности переключения выбираются среди прямых вида: $\kappa_2 \dot{\alpha}_1 + \kappa_2 \alpha_{1\Pi} = 0$ (43), где значение угла $\alpha_{1\Pi}$ определяется формулой:

$$\alpha_{1\Pi} = \begin{matrix} \alpha_1 - \alpha_н \\ 0 \\ \alpha_1 + \alpha_н \end{matrix} \Bigg\} \begin{matrix} \alpha_1 > \alpha_н \\ -\alpha_н \le \alpha_1 \le \alpha_н \\ \alpha_1 < -\alpha_н \end{matrix} \qquad (44)$$

Рациональным выбором коэффициентов усиления κ_1, κ_2 и $\alpha_н$, M удается обеспечить весьма слабую зависимость управляемого относительного движения троса и корабля от начальных условий и длины троса, исключив тем самым появления заматывания троса на корабль и появление больших скоростей соударения космонавта с кораблем.

На рис. 8 изображен один из процессов изменения угла α_1 между тросом и кораблем в случае, когда параметры системы имеют значения:

$\kappa_1 = 1$ $\kappa_2 = 2$ сек $r_{20} = 25$м $M = 10$ кГм $\alpha_н = 0{,}5°$ $r_2(T) = 0{,}5$м

Сравнение свойств управляемого и неуправляемого движения позволяет сделать вывод о плодотворности принятого выхода к синтезу системы управления относительным движением троса и корабля.

ЛИТЕРАТУРА

1. C.R. Poli and E.P. Hanavan. A Three-Mass Retrieval Study for the Gemini Tethered Astronaut. The Journal of the Astronautical Sciences vol XIII N°2 March-April 1966.

2. C.R. Poli. A Study of Retrieval Techniques For Tethered Astronauts. SEG-TDR-65-30, Syst. Eng. Group, Research and Technology Division, Wright-Patterson Air Force Base, Ohio.

3. А.И. Лурье. Аналитическая механика ФМ.Москва,I96I г.

4. В.В. Голубев. Лекции по аналитической теории дифференциальных уравнений ГИТТЛ, I950 г.

5. Ф. Трикоми. Дифференциальные уравнения ИИЛ. Москва,I962.

6. Э.А. Коддингтон и Н. Левинсон. Теория обыкновенных дифференциальных уравнений. ИИЛ. Москва,I958г.

7. С.В. Емельянов. Системы автоматического управления с переменной структурой. Издательство "Наука",Москва,I967 г.

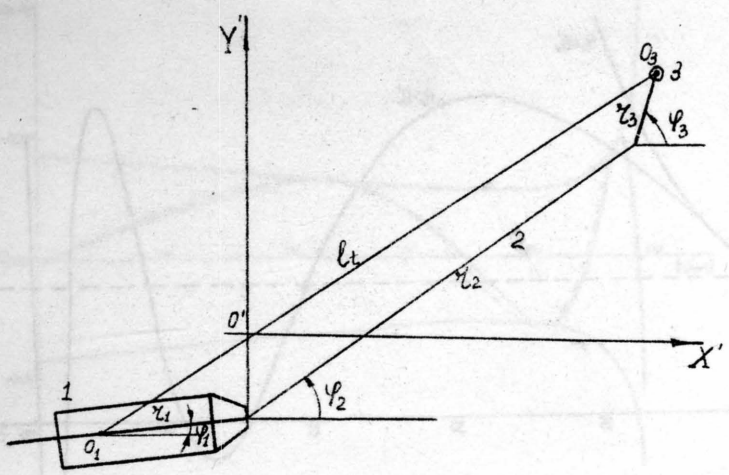

Рис. I. Схема системы и обобщенные координаты.

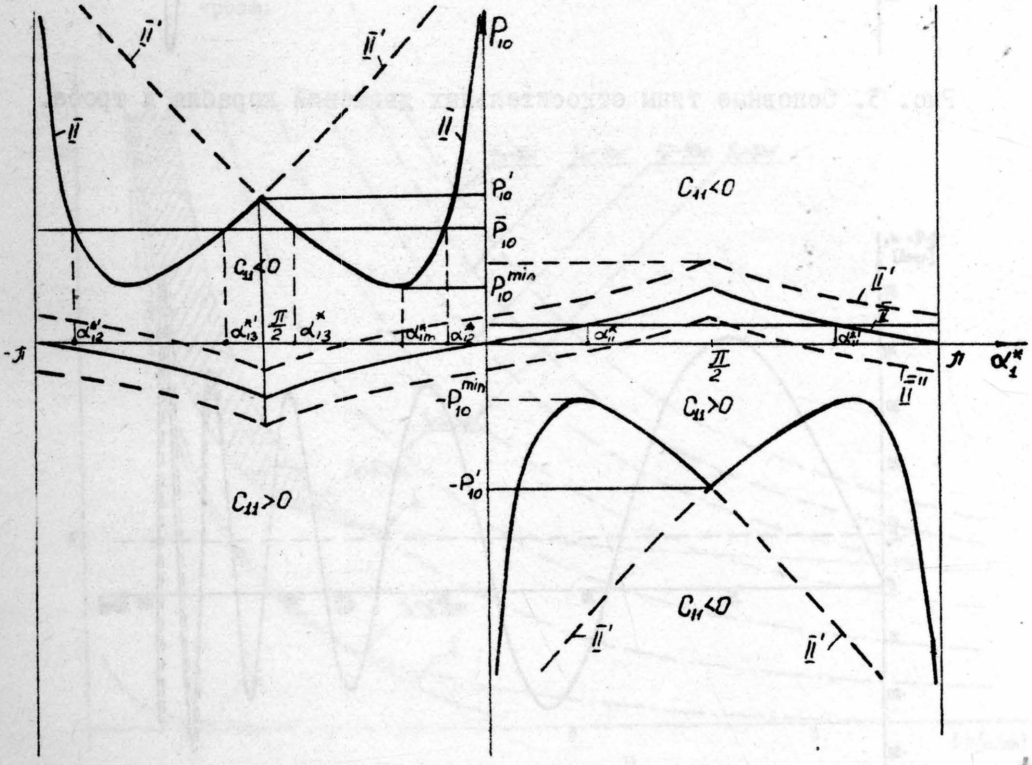

Рис. 2. Бифуркационная диаграмма.

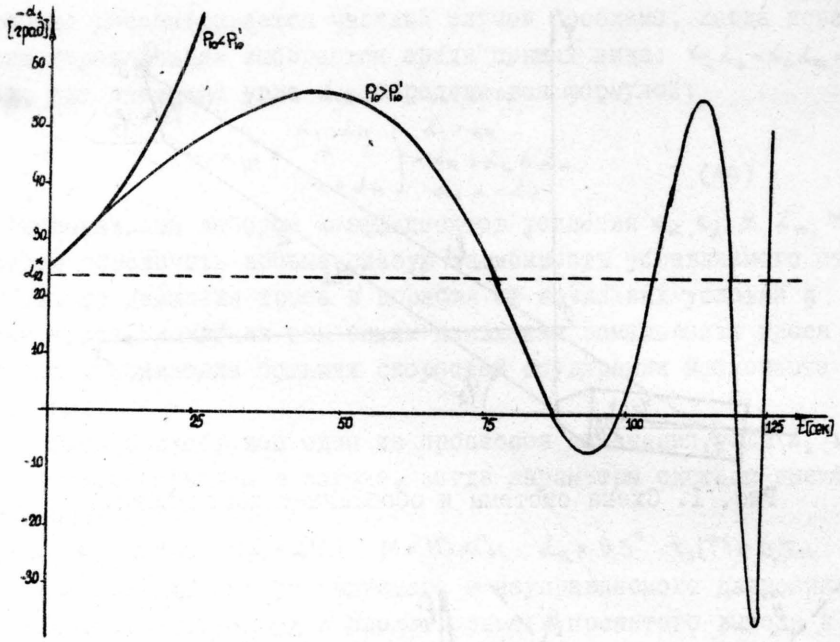

Рис. 3. Основные типы относительных движений корабля и троса.

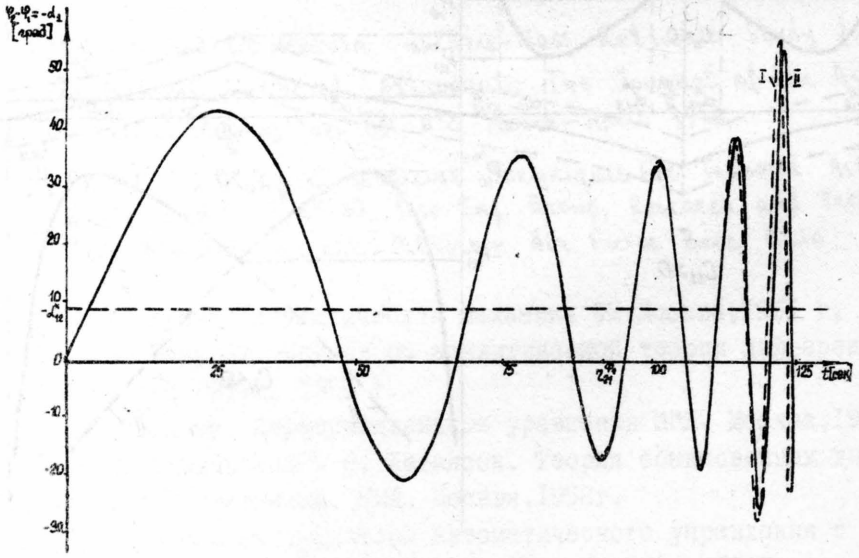

Рис. 4. Колебательные решения нелинейной и приближенной линейной системы для относительного движения корабля и троса.

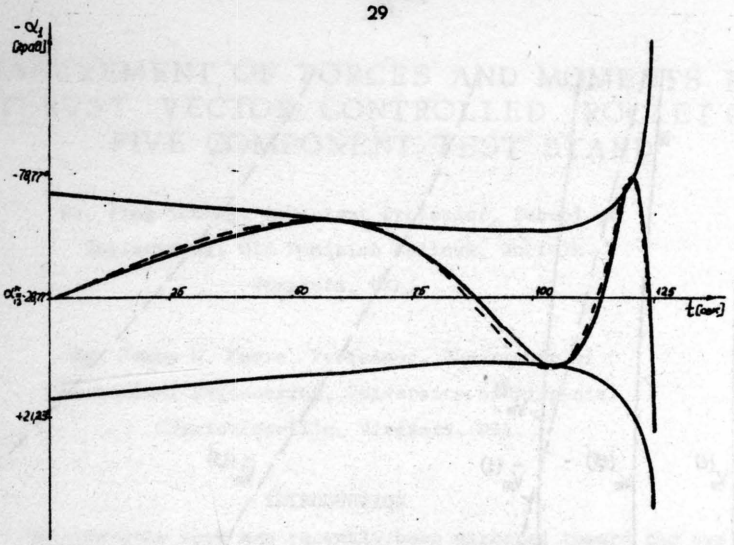

Рис. 5. Асимптотическое представление и точное решение линейного уравнения для относительного движения корабля и троса.

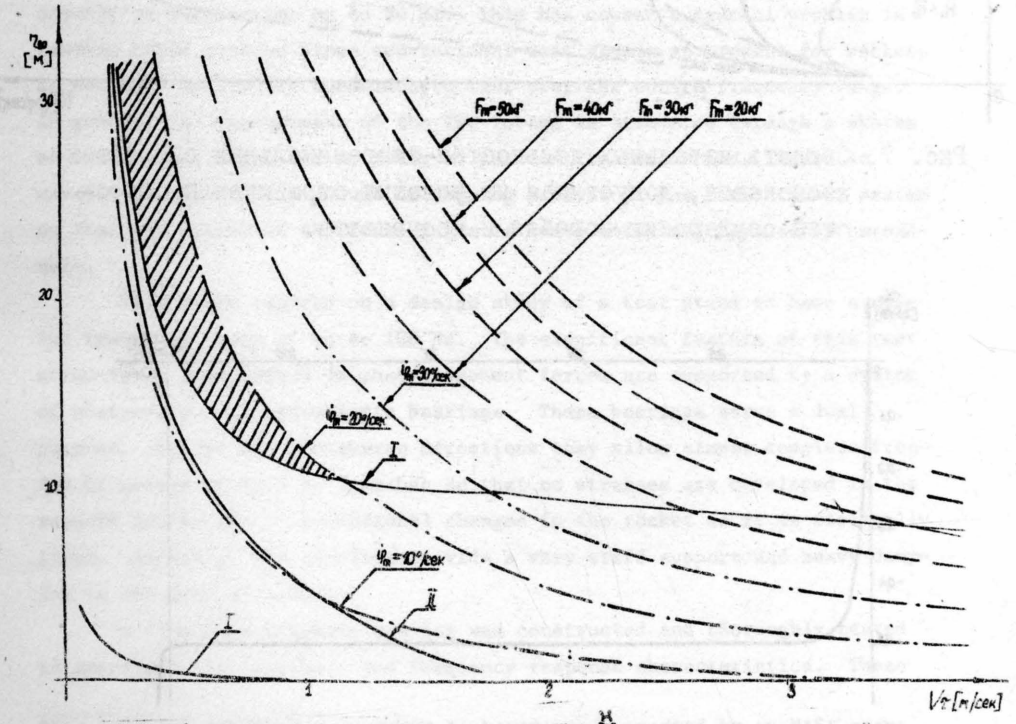

Рис. 6. Область начальных дальностей-тангенциальных скоростей космонавта, допустимая без учета ограничений на скорость соударения корабля и космонавта.

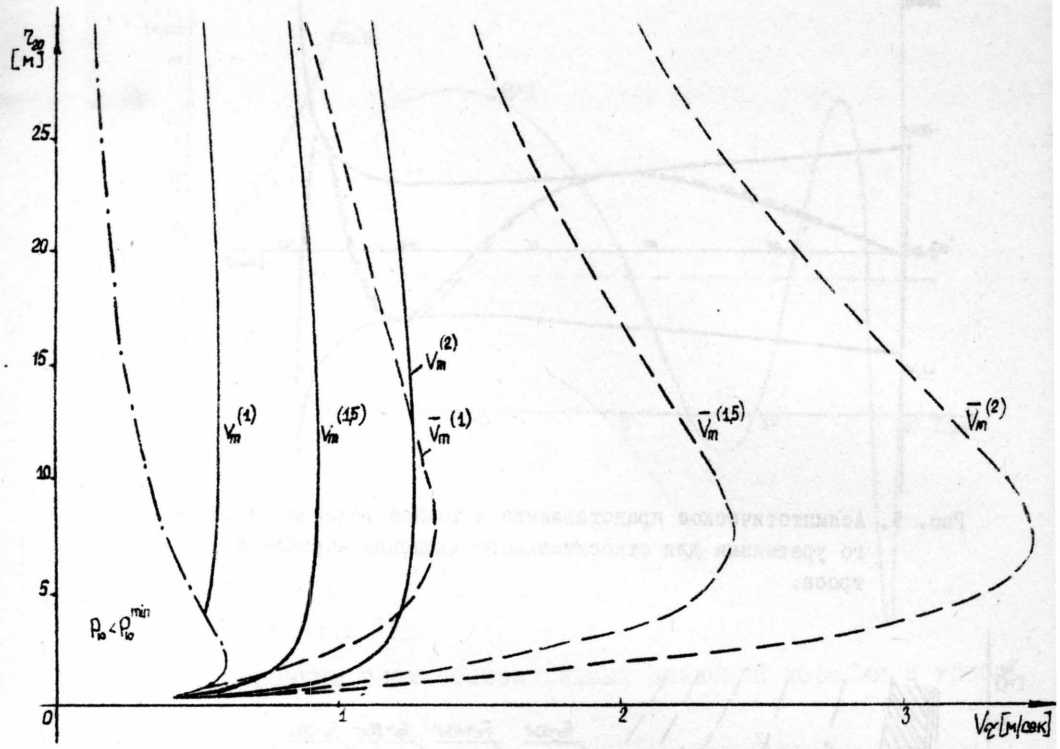

Рис. 7. Область начальных дальностей–тангенциальных скоростей космонавта, допустимая из условия ограничения скоростей соударения корабля и космонавта.

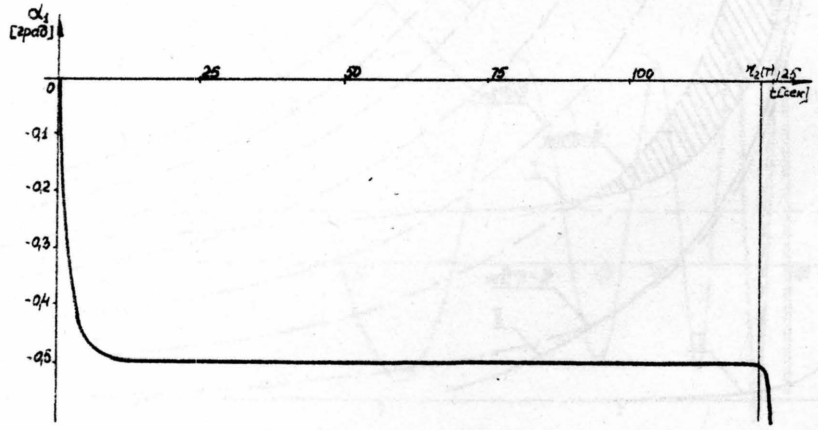

Рис. 8. Относительное движение корабля и троса для одного типа управления кораблем.

MEASUREMENT OF FORCES AND MOMENTS FROM A THRUST VECTOR CONTROLLED ROCKET ON A FIVE COMPONENT TEST STAND*

Dr. Ping Tcheng, Assistant Professor, School of Engineering, Old Dominion College, Norfolk Virginia, USA.

Dr. James W. Moore, Professor, Department of Mechanical Engineering, University of Virginia Charlottesville, Virginia, USA.

INTRODUCTION

Considerable work has recently been directed toward the use of thrust vector control (TVC) for the purpose of steering rockets. Since there are no heavy masses of metal to move in the TVC system it is possible to attain much higher bandwidth on the control signal. One such system appears to be capable of frequencies up to 80 Hz. This has caused a special problem in testing these systems since conventional test stands at present for rockets do not have sufficient bandwidth to test over the entire frequency range. In general the measurement of the TVC forces is attempted through a system of force gages which are an integral part of the test stand. There is usually no appreciable amount of damping present in the conventional system so that the output of the force gages is quite noisy and frequently unreadable.

This paper reports on a design study of a test stand to have a useful frequency range of up to 100 Hz. The significant feature of this test stand-force gage system is that component forces are supported by a system of pressurized oil hydrostatic bearings. These bearings serve a dual purpose. In the two transverse directions they allow almost complete freedom of motion up to 1 to 2 inches so that no stresses are developed in the support system due to dimensional changes in the rocket as it is statically fired. Secondly, the bearings provide a very stiff support and heavy damping in the load direction.

A five-inch diameter bearing was constructed and thoroughly tested to ascertain its stiffness and frequency response characteristics. These

*The research on which this paper is based was supported by an NASA grant from the Force Measurements Section of the Instrument Research Division of NASA, Langley Field, Virginia on Grant NGR 47-005-026.

tests indicate that it behaves almost exactly as a first order lag filter so that an equivalent spring rate and damping coefficient can be calculated.

The TVC rocket test stand proposed here is a system of six hydrostatic bearings, six force gages, and a base. Dynamic studies have been made on the digital computer using bearing data and rocket characteristics. The results indicate the feasibility of a test stand having a flat frequency response to 100 Hz.

DYNAMIC CHARACTERISTICS OF THE SUPPORT MEMBERS

A simple model for the proposed rocket test stand is shown diagrammatically in Fig. 1. Six support members are used. Each support member consists of a hydrostatic oil bearing and a force gage placed in series as shown in Fig. 2. The oil bearing provides the stiffness and damping required to support the rocket motor and the force gage is used to measure the force transmitted through the support member.

A. HYDROSTATIC OIL BEARING

The experimental frequency responses of a hydrostatic oil bearing from a prototype model developed at the University of Virginia[1] indicate that the bearing can be assumed to be composed of a spring and a viscous damper placed in parallel. The assumption has been verified by theory[2]. Based on this theory, a ten-inch diameter hydrostatic oil bearing with multi-pocket, opposite-pad has been proposed[3]. The bearing transfer function from the bearing displacement to the input force is of the form

$$A(s) = \frac{F_b(s)}{X_b(s)} = K_b + C_b S \tag{1}$$

where $K_b = 4.4 \times 10^6$ lb/in and $C_b = 1.33 \times 10^4 \frac{\text{lb-sec}}{\text{in}}$ which are calculated from theory [2].

B. FORCE GAGE

The force gage considered is a commercially available load cell specially designed for the sensing of dynamic forces. The spring stiffness is given as $K = 2.7 \times 10^7$ lb/in.

C. HYDROSTATIC OIL BEARING--FORCE GAGE ASSEMBLY

The schematic diagram of the assembly is shown in Fig. 3. The transfer function of the assembly is formed as

$$A_1(s) = F_b(s)/K_b(s) = K\ell(s + B_p)/(s + B_Q) \qquad (2)$$

where $B_p = K_b/C_b$ and $B_Q = (K_b + K\ell)/C_b$.

TEST STAND MODEL AND DYNAMIC RESPONSES

The model of the proposed rocket test stand that uses the support members described in the previous section is not analyzed. For the present, only motion in the yaw plane due to TVC force is considered. Cross-couplings between orthogonal planes are ignored here since the bearings help eliminate them. Cross-couplings are termed as errors and will be considered in the next section.

A. TEST STAND MODEL

The model used for this analysis as shown Fig. 1 conforms dimensionally to a test stand which has been used. Propellant weight and burning rate are those for rockets which have been tested. Because of the burning of propellant in the rocket motor, the rocket and test stand form a system which can be best described by differential equation with time-varying parameters. The effect of these time-varying parameters is considered at discrete intervals in time, as the rocket burning progresses. Before formulation of the differential equations which describe the motion of the model, it is necessary to define the parameters of the model. The calculations of the time-varying parameters are summarized in Table 1. It should be noted that end to end burning of the propellant is assumed.

B. EQUATIONS OF MOTION OF THE SYSTEM

The equations of motion for the system in the yaw plane may now be written. Letting x be the displacement of the center of mass of the system and θ the rotation about the center of mass as shown in Fig. 1, and by considering that the test stand is supported by front and rear struts with transfer functions $A_1(s)$ and $A_2(s)$ respectively, the Laplace transformed equations of motions of the system can be derived by Newton's second law of motion to be as follows

$$M_s s^2 X(s) + [X(s) - \ell_1\ (s)]\ A_1(s) + [X(s) + \ell_2\ (s)]\ A_2\ (s) = F(s)$$

$$J_s s^2\ (s) - [X(s) - \ell_1\ (s)]\ \ell_1 A_1(s) + [X(s) + \ell_2\ (s)]\ \ell_2 A_2(s) = F(s)\ell_3 \qquad (3)$$

where $A_1(s) = K\ell(s+B_p)\ /\ (s+B_Q)$ and $A_2(s) = 2A_1(s)$ since two parallel bearing and force gage assemblies are considered for the rear strut.

The transfer functions from the applied force F(s) to the force gage reading in the front and rear supports are found by solving Eq. (3) as

$$F_1(s)/F(s) = K\ell(s + B_p)\, P_1(s)/P(s),$$
$$F_2(s)/F(s) = K\ell(s + B_p)\, P_2(s)/P(s), \qquad (4)$$

where

$$P(s) = M_s J_s s^4(s + B_Q)^2 + K\ell s^2[3J_s + M_s(\ell_1 2 + 2\ell_2{}^2)]\ (s + B_p)$$
$$(s + B_Q) + 2\ell^2 K\ell^2(s + B_p)^2,$$
$$P_1(s) = (J_s - M_s\ell_1\ell_3)s^2(s + B_Q) + 2K\ell\ell(\ell_2 - \ell_3)(s + B_p),$$
$$P_2(s) = (J_s + M_s\ell_1\ell_3)s^2(s + B_Q) + K\ell\ell(\ell_1 + \ell_3)(s + B_p).$$

C. SYSTEM RESPONSES

Frequency Response

By setting $s = \omega j$, Eq. (4) can be evaluated to give the front and rear force gage reading as a function of frequency, for a unit-amplitude sinusoidal force input. This amounts to determining the test stand frequency response. This operation was carried out by employing a digital computer.

The computed frequency responses of the test stand are now presented. Figs. 4 and 5 show the normalized front and rear force gage readings, as a function of the input frequency of the applied thrust vector controlled force.

The desired output from the test stand is a measure of the input force F(s), that is, the thrust vector controlled force. Statically, the applied force is the sum of the forces in the support members. Thus, the sum of the outputs of the three force gages over the input force,

$$F_R(s)/F(s) = [F_1(s) + 2F_2(s)]/F(s)$$
$$= K\ell(s + B_p)\ [P_1(s) + 2P_2(s)]\ /\ P(s) \qquad (5)$$

will be unity for $s = 0$. Fig. 6 show Eq. (5) as a function of the input frequency. Both of the frequency responses at the initial burning time $t = 0$ and at the final burning time $t = 46$ sec are plotted from Figs. 4 to 6; however, the latter curves are broken in the low frequency range whenever they become indistiguishable from the former ones. Although the upper bounded frequency of interest is 100 Hz, frequencies up to 1000 Hz are presented in order to obtain a better understanding of the test stand dynamics.

Transient Response For A Step Input

The transient responses of the system, that is, the time response of Eq. (5), were obtained through a simulated test stand model on an analog computer. Fig. 7 shows the sum of the three force gages transient response from an applied TVC force of 350 lb.

Dynamic Response Inprovement

Judging from the transient response of the reconstructed TVC force shown in Fig. 7, it was considered that a low-pass filter could be used to improve the dynamics of the recorded output from the test stand. A low-pass filter in the form of $\frac{1}{1+RCs}$ with a break frequency of 300 Hz was chosen. The filtered transient response and frequency response of the reconstructed TVC force are shown in Figs. 8 and 9, respectively.

DISCUSSION OF ERRORS

The error in measuring thrust vector controlled force F and moment $F\ell^4$ due to interactions between orthogonal planes of the test stand are presented. As may be expected, a major source of error comes from the misalignment of the rocket motor. The loading of a heavy rocket motor to a predetermined perfect position is extremely difficult. Even then, the asymmetry of test stand introduces force gage reading errors.

In short, the three main sources of error considered are:

(1) Viscous drags within the hydrostatic oil bearing,

(2) Misalignments of the rocket motor,

(3) Reactional moments in the bearing-force gage assemblies.

Both the static and dynamic effects and the amount of each of the above errors are given. Steps are taken to eliminate these errors in the data acquisition process if they are not tolerable.

A. FORCE MEASUREMENT ERROR

Force measurement errors resulted from the various sources are tabulated in Table 2. The details can be found in reference [3].

B. MOMENT MEASUREMENT ERROR

It was shown in reference [3] that the moment measurement error equals to the force measurement error in the rear force gages.

DISCUSSIONS AND CONCLUSIONS

Both the frequency response and the transient response of the reconstructed trust vector controlled force F_R are satisfactory. The resonant frequency is well beyond the desired value of 100 Hz and the resonant peak value of slightly greater than 2 is not high. The transient response shows a fast rise time and tolerable amount of overshoot. As the rocket motor burning progresses, there is only negligible change in the frequency response of F_R for the low frequency range, while slight change is seen for frequencies higher than 100 Hz. Variation of the transient response of F_R as a function of time is seen in Fig. 7; however, these responses are all quickly settled in less than 6 milliseconds.

It was found that viscous drags within the hydrostatic oil bearing are negligible. This implies that resulting cross couplings between different orthogonal planes are negligible.

It is also found that with careful alignment, that is, if the center of gravity and the geometrical center line of the rocket motor is set within 0.5 inch to each other, the magnitudes of errors induced by the misalignments are acceptable.

The influence of the tilting resistance from the oil bearing on the accuracy of the reconstructed TVC force reading is negligible.

The last two kinds of force reading errors can be eliminated completely by a simple data reduction technique in which the readings of all three force gages in the yaw plane are summed.

The accuracy of measuring input moment in the yaw plane depends upon the accuracy of the measured outputs of the two rear force gages in the same plane. The rear force gage reading $R_2(s)$ is contaminated by a D-C value as a result of sinusoidal signal from F and a D-C signal from Te_x after the transient dies out. These two signals are distinguishable. The true amplitude of the sinusoidal part of $F_2(s)$ can thus be recovered. Therefore, the reconstructed moment in the yaw plane becomes identical to the applied moment.

BIBLIOGRAPHY

1. McVey, E. S., J. W. Moore, et al., "Final Report on Rocket Engine Test Stand Design Information," NASA Report No. EME-4029-105-67U, Research Laboratories for the Engineering Sciences, University of Virginia, Charlottesville, December 1967.

2. Wilcock, D. F., "Externally Pressurized Bearings as Servomechanisms. 1--The Simple Thrust Bearing," Trans. ASME, Vol. 89. Series F, No. 4, October 1967.

3. Tcheng, P., "Measurement of Forces and Moments From A Thrust Vector Controlled Rocket by Means of Five-Component Test Stand," Doctoral Dissertation, University of Virginia, Charlottesville, August 1968.

NOMENCLATURE

$A(s)$	= bearing transfer function, Laplace transformed.
$A_1(s)$, $A_2(s)$	= bearing-force gage assembly's transfer function, Laplace transformed.
B_P, B_q	= break frequency of transfer function $A_1(s)$, $A_2(s)$.
C	= filter capacitance farad.
C_b	= bearing damping coefficient, lb-sec/in.
F	= TVC force, lb.
$F(s)$	= TVC force, Laplace transformed.
$F_b(s)$	= bearing forcing input, Laplace transformed.
$F_F(s)$	= reconstructed TVC force after filtering, Laplace transformed.
F_R	= reconstructed TVC force, lb.
$F_R(s)$	= reconstructed TVC force, Laplace transformed.
$F_1(s)$, $F_2(s)$	= force gage reading, Laplace transformed.
J_s	= rocket motor moment of inertia, slug-ft^2.
K_b	= bearing stiffness, lb/in.
$K\ell$	= force gage stiffness, lb/in.
M_s	= rocket motor mass, slug.
$P(s)$, $P_1(s)$, $P_2(s)$	= expression used in evaluation force gage reading, Laplace transformed.
R	= filter resistance, ohm.
$X(s)$, $Y(s)$, $Z(s)$	= linear coordinate displacement, in., transformed.
$X_b(s)$	= bearing displacement, Laplace transformed.
j	= $\sqrt{-1}$
ℓ, ℓ_1, ℓ_2, ℓ_3, ℓ_4	= distance, ft.
s	= Laplace operator, sec^{-1}.
t	= rocket motor ignition time, sec.
x, y, z	= linear coordinate displacement, in.
$\Theta(s)$, $\Psi(s)$, $\Phi(s)$	= angular coordinate displacement, Laplace transformed.
θ Ψ Φ	= angular coordinate displacement, rad.
ω	= frequency, rad/sec.
ω_n	= natural frequency, rad/sec.

TABLE 1

NUMERICAL VALUES OF SYSTEM PARAMETERS

t sec	M_s slug	J_s slug-ft	ft	ft	ft
0	62.2	139.0	2.280	0.873	2.655
5	60.3	137.6	2.258	0.895	2.677
10	58.4	136.9	2.246	0.907	2.689
20	54.7	135.9	2.255	0.898	2.680
30	51.0	132.2	2.315	0.838	2.262
40	47.3	121.3	2.439	0.714	2.496
46	45.0	109.3	2.547	0.606	2.388

TABLE 2

FORCE MEASUREMENT ERRORS

SOURCE OF ERROR		INDUCED ERRONEOUS MOTION OR READING	MAXIMUM MAGNITUDES OF ERRONEOUS MOTION OR READING	METHOD OF ERROR ELIMINATION
Viscous Drag		frictional force opposite to the motion of the system	0.012% error in Thrust Vector Controlled force Measurement	none, but the magnitude of error is negligible
Misalignment (0.5 inch, maximum)	Misalignment component in z-direction	damped sinusoidal motion in roll plane	270 Hz, additional deflection in the two aft supports is 5.4% of its static value from TVC	completely eliminated by summing two aft force gage readings
	Misalignment component in x-direction	stepped responses in yaw plane	additional deflection in the front & aft supports are 26% & 9% of its static values from TVC, respectively	completely eliminated by summing the two aft and one front force gage readings
Tilting Motion	Static Case	force gage reading errors due to additional torque generated within the hydrostatic oil bearing	2.3% & 1% error in front & aft force gage readings, respectively	
	Dynamic Case		no additional dynamic error involved	

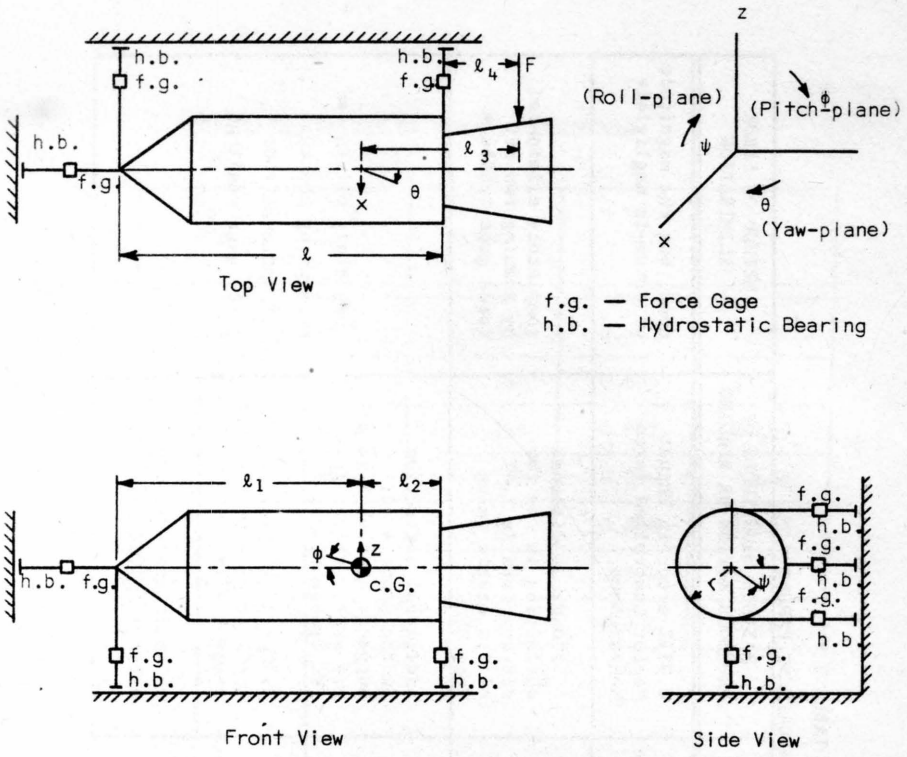

Fig. 1 Physical Model of the Rocket Motor Test Stand System

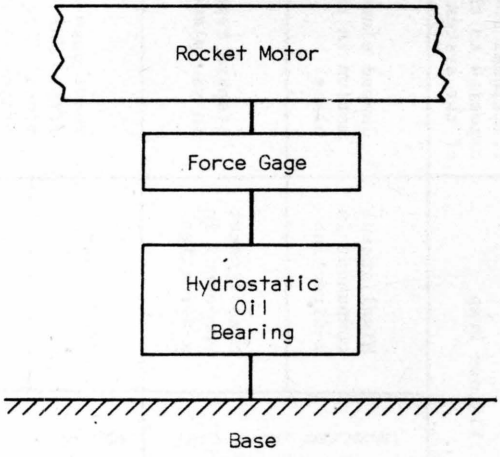

Fig. 2 Schematic Diagram of Bearing-Force Gage Assembly

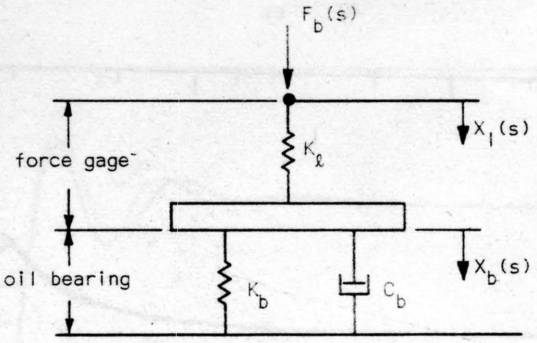

Fig. 3 Bearing Force Gage Assembly

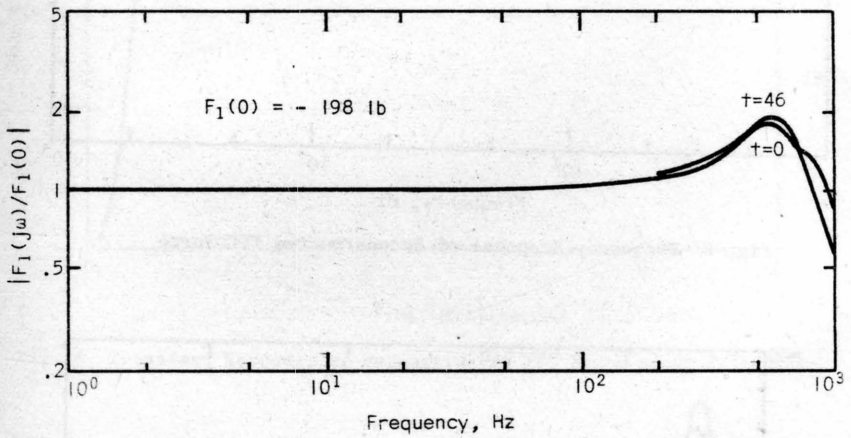

Fig. 4 Frequency Response of Normalized Front Force Gage Reading

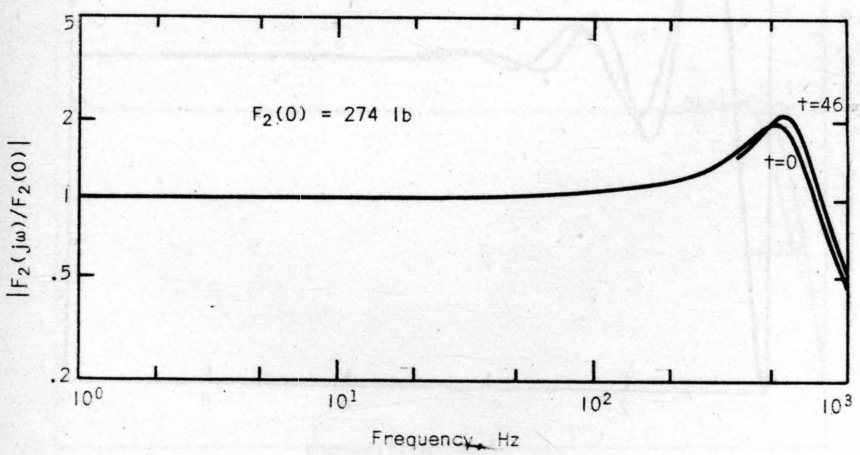

Fig. 5 Frequency Response of Normalized Rear Force Gage Reading

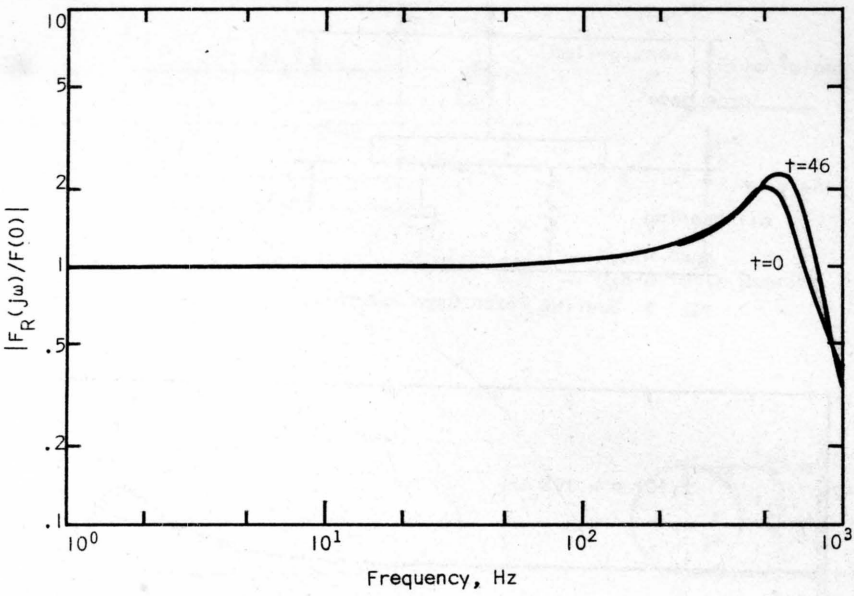

Fig. 6 Frequency Response of Reconstructed TVC Force

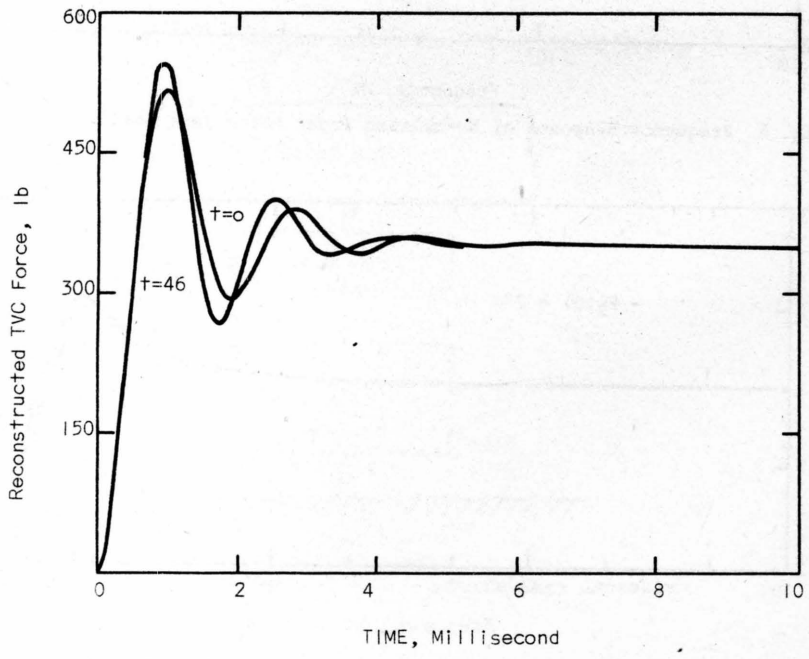

Fig. 7 Transient Response of Reconstructed TVC Force

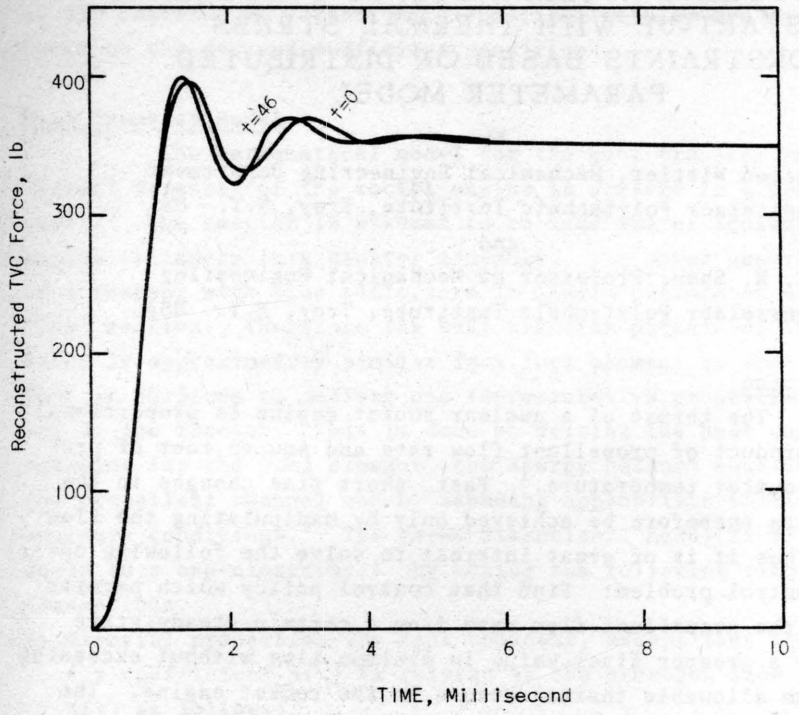

Fig. 8 Transient Response of Reconstructed TVC Force after Filtering

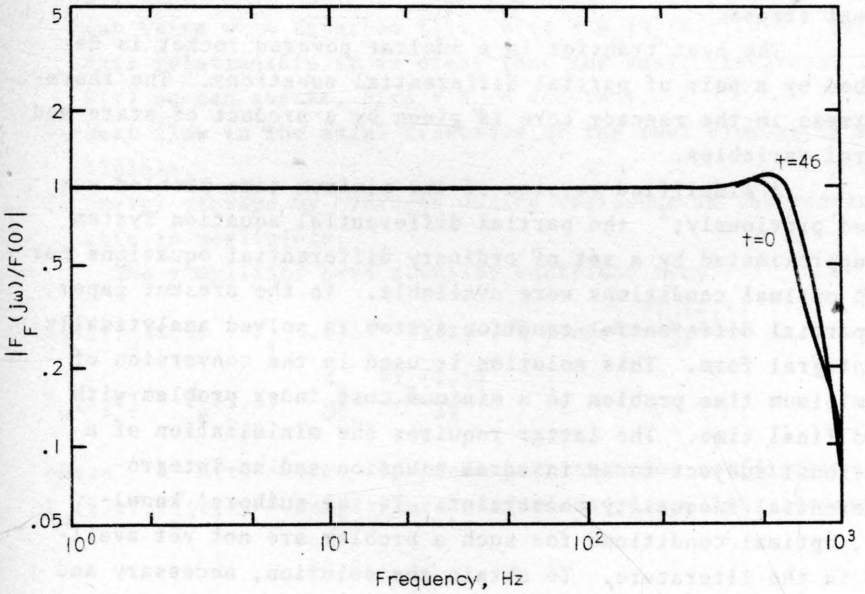

TIME-OPTIMAL NUCLEAR ROCKET PROPELLANT START-UP WITH THERMAL STRESS CONSTRAINTS BASED ON DISTRIBUTED PARAMETER MODEL

by

Manfred Wittler, Mechanical Engineering Department
Rensselaer Polytechnic Institute, Troy, N.Y. USA

and

C. N. Shen, Professor of Mechanical Engineering
Rensselaer Polytechnic Institute, Troy, N.Y. USA

Introduction

The thrust of a nuclear rocket engine is proportional to the product of propellant flow rate and square root of propellant outlet temperature.[1] Fast, short time changes in the thrust can therefore be achieved only by manipulating the flow rate. Thus it is of great interest to solve the following optimal control problem: Find that control policy which permits raising the propellant flow rate from a certain steady-state value to a greater final value in minimum time without exceeding a maximum allowable thermal stress in the rocket engine. The thermal stress constraint is introduced because nuclear rocket engines operate at very high core temperatures and with steady-state thermal stresses very close to the maximum allowable thermal stress.

The heat transfer in a nuclear powered rocket is described by a pair of partial differential equations. The thermal stress in the reactor core is given by a product of state and control variables.

A simplified version of the minimum time problem was solved previously;[2] the partial differential equation system was approximated by a set of ordinary differential equations for which optimal conditions were available. In the present paper, the partial differential equation system is solved analytically in integral form. This solution is used in the conversion of the minimum time problem to a minimum cost index problem with fixed final time. The latter requires the minimization of a functional subject to an integral equation and an integro-differential inequality constraint. To the authors' knowledge, optimal conditions for such a problem are not yet available in the literature. To obtain the solution, necessary and some sufficient conditions are derived for this problem with the aid

of the calculus of variations. Numerical results are obtained based on the derived sufficient conditions.

Heat Transfer Model

The mathematical model for the heat transfer and the thermal stresses of the rocket engine is derived in a previous paper.[3] The reactor is assumed to be made out of equivalent hollow cylinders in a cluster assembly. The power generation of a reactor with side reflectors is nearly uniform in each cross section. Therefore the heat transfer pattern of the reactor is approximately similar from fuel element to fuel element. Thus it suffices to analyze one representative propellant channel of the reactor. This is done by writing the heat conduction equation for the fuel element, the energy balance equation for the propellant channel and by assuming appropriate initial and boundary conditions.[3] The three-dimensional model is then reduced to a one-dimensional by making the following simplifying assumptions.

a) Material properties are kept constant, except that the heat transfer coefficient $h(\tau)$ is related to the hydrogen flow rate $W(\tau)$ as follows.[4]

$$h(\tau)/h_o = [W(\tau)/W_o]^{0.8} \qquad (1)$$

where h_o, W_o = reference heat transfer coefficient and hydrogen flow rate. Let $\beta_o = h_o/W_o$ and $\beta(\tau) = h(\tau)/W(\tau)$. Then we can write with Equation (1): $\beta(\tau) = \beta_o[W_o/W(\tau)]^{0.2}$. From this relationship it is clear that for small variations in $W(\tau)$ we can assume, $\beta(\tau) \simeq \beta_o$ = constant.

b) Heat flow in the axial direction of the fuel element is negligible.

c) Energy storage by hydrogen during residence in the reactor core is negligible.

The simplified heat transfer equations are,[3]

$$h(\tau)[T_u(z,\tau) - T_g(z,\tau)] = P_1(z,\tau)b^* - \rho cb^*\eta\frac{\partial T_u(z,\tau)}{\partial \tau} \qquad (2)$$

$$T_u(z,\tau) - T_g(z,\tau) = \frac{c_g}{D\beta_o}\frac{\partial T_g(z,\tau)}{\partial z} \qquad (3)$$

where $h(\tau)$ = time dependent heat transfer coefficient

$T_u(z,\tau), T_g(z,\tau)$ = temperature of fuel and propellant respectively

$P_1(z,\tau)$ = fission energy generation per unit volume

ρ, c = density and specific heat of fuel

$c_g, W(\tau)$ = specific heat and mass flow rate of propellant

τ = independent variable time

z = independent variable channel position

D = perimeter of hydrogen channel

b^* = equivalent half thickness of fuel element

η = weighting factor between the mean temperature in the transverse direction and the surface temperature of the fuel element.

The following transformation of variables is introduced.

$$Z = D\beta_o z/c_g \; ; \; Z\varepsilon[0,L] \quad ; \quad t = \tau/\rho c b^* \eta \; ; \; t \geq 0 \tag{4}$$

where L denotes the transformed length of the reactor. The transformation (4) simplifies the partial differential equations.

Equations (2) and (3) may be written as;

$$\frac{\partial T_u(Z,t)}{\partial t} = P(Z,t) - h(t)[T_u(Z,t) - T_g(Z,t)] \tag{5}$$

$$\frac{\partial T_g(Z,t)}{\partial Z} = T_u(Z,t) - T_g(Z,t) \tag{6}$$

where $P(Z,t) = P_1(Z,t)b^*$. One boundary condition is given.

$$T_g(Z,t)\big|_{Z=0} = T_{go} = \text{constant} \tag{7}$$

That is, the propellant temperature at the reactor entrance is constant. The following initial condition (8) is derived from Equations (5) and (6) under the assumption that the rocket engine was operating at steady-state prior to t=0.

$$T_u(Z,t)\big|_{t=0} = T_{go} + \frac{1}{h_o}\left[P_o(Z) + \int_o^Z P_o(w)dw\right] \tag{8}$$

where $P_o(Z) = P(Z,t)$ for $t \leq 0$. Equations (5) and (6) may be combined to give a second order partial differential equation for T_u, T_g or Θ respectively, where the latter is defined as follows,

$$\Theta(Z,t) = T_u(Z,t) - T_g(Z,t) \tag{9}$$

All of these second order equations have the same general form with y standing for T_u, T_g or Θ.

$$\frac{\partial^2 y(Z,t)}{\partial Z \partial t} + \frac{\partial y(Z,t)}{\partial t} + h(t)\frac{\partial y(Z,t)}{\partial Z} = f(Z,t) \tag{10}$$

The forcing term $f(Z,t)$ depends on the power generation: $f(Z,t)$ has a different form for y representing T_u, T_g or Θ respectively. The solution of Equation (10) is obtained in integral form by Laplace transforming the equation with respect to Z. The resulting ordinary differential equation in the time domain is easily solved and the inverse transform can be taken.[1]

$$y(Z,t) = \int_0^t \int_0^Z R_1[\tau,\xi,u(\tau),u(t),Z]\,d\xi\,d\tau + \int_0^t R_2[\tau,u(\tau),u(t),Z]\,d\tau + \int_0^Z R_3[\xi,u(t),Z]\,d\xi + R_4[u(t),Z] \tag{11}$$

where

$$R_1[\tau,\xi,u(\tau),u(t),Z] = f(Z-\xi,\tau)I_o(2\sqrt{\xi[u(t)-u(\tau)]})e^{-u(t)+u(\tau)-\xi} \tag{12}$$

$$R_2[\tau,u(\tau),u(t),Z] = \left[\frac{\partial y(Z,\tau)}{\partial \tau}\bigg|_{Z=0} + h(\tau)y(0,\tau)\right] \cdot I_o(2\sqrt{Z[u(t)-u(\tau)]})e^{-u(t)+u(\tau)-Z} \tag{13}$$

$$R_3[\xi,u(t),Z] = \left[\frac{\partial y(\alpha,0)}{\partial \alpha}\bigg|_{\alpha=Z-\xi} + y(Z-\xi,0)\right]I_o(2\sqrt{\xi u(t)})e^{-u(t)-\xi} \tag{14}$$

$$R_4[u(t),Z] = y(0,0)I_o(2\sqrt{Zu(t)})e^{-u(t)-Z} \tag{15}$$

The symbol I_o represents the modified Bessel function of zero order, and the function $u(t)$ is defined as follows,

$$u(t) = \int_0^t h(w)\,dw \tag{16}$$

The forcing function and all initial and boundary values appearing in Equations (12) through (15) can be determined from Equations (5) through (8). Thus the Equation (11) gives an explicit solution for the core temperature $T_u(Z,t)$, the propellant temperature $T_g(Z,t)$ and the difference $\Theta(Z,t)$.

Thermal Stress Model

A detailed treatment of the thermal stress problem is found in the previous paper.[3] Since the axial length of the fuel element is larger than the transverse direction, the plane-strain formulae for thermal stresses were employed. The maximum

thermal stresses in each cross section were found to be at the intersurface of the fuel element, and could be expressed in terms of the temperature gradient at this location. The final formula for transient thermal stresses was given as,

$$\sigma(z,\tau) = C_1 h(\tau)[T_u(z,\tau) - T_g(z,\tau)] \tag{17}$$

where $\sigma(z,\tau)$ = thermal stress at position z and time τ

C_1 = constant depending on the geometry and material properties.

We are only interested in the thermal stress at the position where the stress has its largest value with respect to all other positions. Thus, making use of Equations (4), (9) and (17) the maximum thermal stress is given by,

$$\sigma_{max}(t) = C_1 h(t) \max_{Z\varepsilon[0,L]} \Theta(Z,t) \tag{18}$$

Formulation of the Time-Optimal Control Problem

The thrust of a rocket is proportional to the product of propellant flow rate and square root of propellant temperature at the reactor exit. Propellant flow rate and power generation are the two input variables of the reactor. Changes of the propellant outlet temperature due to these input variables are delayed through the system dynamics. This is the reason that a fast, short time increase in thrust can be achieved only by manipulating the flow rate.

Fast transients in the flow rate cause high thermal stresses. Due to limitations in the strength of the structural material, all thermal stresses must not exceed a maximum tolerable limit. Nuclear rocket engines operate at very high core temperatures with steady-state stresses very close to the maximum allowable thermal stress. Thus it is clear that the flow rate transients must be constrained by the condition that a certain stress limit should not be exceeded, i.e.

$$\sigma_{max}(t) = C_1 h(t)\Theta(t) \leq \sigma_{limit} \tag{19}$$

where

$$\Theta(t) = \max_{Z\varepsilon[0,L]} \Theta(Z,t) \tag{20}$$

The optimal problem will be formulated in terms of the heat transfer coefficient because the ratio of propellant flow

rate to heat transfer coefficient is assumed to be constant. Then the minimum time problem can be stated as follows: Find that control policy which permits raising the heat transfer coefficient h(t) (control variable) from its steady-state value h_o to a greater final value h_f in minimum time without violating the inequality constraint (19).

In the above problem the stopping condition is given by,

$$h(t_f) = h_f \tag{21}$$

That is, the final time t_f is determined by the control variable reaching the value h_f. The problem formulation with such a stopping condition makes sense only if the set of admissible controls is defined by constraints which are dependent on the state of the control system. Here, this constraint is given by Equation (19). If this constraint were removed the problem would be trivial: one could step the control from the initial value h_o to the desired final value h_f in zero time.

Conversion to Equivalent Fixed Final Time Problem

Writing the inequality (19) differently and introducing a lower limit for the heat transfer coefficient gives,

$$0 \leq a \leq h(t) \leq C/\Theta(t) \tag{22}$$

where $C = \sigma_{limit}/C_1$. The inequality (22) must be satisfied for all times t including the minimal time t_f. Substituting the stopping condition (21) into the inequality (22) gives a final condition on the function $\Theta(t)$ which must be satisfied by the minimum time control.

$$\Theta(t_f) \leq C/h_f \tag{23}$$

The function $\Theta(t)$ depends only on one manipulated variable, namely the control variable u(t) which was defined as the integral of the physical control h(t) by Equation (16). Assume initially $\Theta_o = \Theta(0) > C/h_f$. Define the region A of the Θ,t-plane as the set of states which can be reached starting from Θ_o by applying all admissible controls to the system, i.e. control policies which do not violate Equation (22). The control policy or policies leading to the lower boundary E of that region may be found

by minimizing $\Theta(t)$ for all fixed values of time $T > 0$. Then the minimum time control policy for the original problem is identical with the control policy leading to that point on the lower boundary E for which $\Theta(t_f) = C/h_f$; this point also defines the minimum time t_f.

It should be emphasized that the control policy generating the lower boundary E must not necessarily lead to $h(t_f) = h_f$. But if $h(t)$ at the minimum time is smaller than h_f one can always jump the control to the value h_f without violating the constraint (22).

From Equation (16) it is seen that the mathematical control function $u(t)$ has an initial value of zero and that the physical control function $h(t)$ is the derivative of the mathematical control function. To be consistent in the following analysis, referring to the control function will always mean reference to the mathematical control $u(t)$. The notation $u'(t)$ is used instead of $h(t)$ to denote the derivative of $u(t)$ and therefore the physical control, the heat-transfer coefficient. The fixed final time problem equivalent to the minimum time problem can now be formed.

Statement of Equivalent Problem

Among all continuous functions $u(t)$, $Z(t)$, $t\varepsilon[0,T]$ which have piecewise continuous first derivatives and which satisfy the initial condition

$$u(0) = 0 \tag{24}$$

find those functions $u^*(t)$, $Z^*(t)$ for which the functional

$$J[u,Z] = \Theta(T) = \Theta[Z(T),T] \tag{25}$$

has a minimum subject to the inequality constraint

$$a \leq u'(t) \leq C/\Theta(t) \quad ; \quad t\varepsilon[0,T] \tag{26}$$

and to the equality constraint

$$\Theta(t) = \Theta[Z(t),t] = \max_{Z\varepsilon[0,L]} \Theta(Z,t) \quad ; \quad t\varepsilon[0,T] \tag{27}$$

where

T = constant

t = independent variable defined on $[0,T]$

$u(t), Z(t)$ = continuous functions for $t\varepsilon[0,T]$

$\Theta(Z,t)$ = function defined by Equation (11).

It should be pointed out that the function Z(t) denotes the position of maximum θ at any time t and is defined through Equation (27). Thus, Equation (27) represents an equality constraint for the minimization problem. If the maximum of θ occurs on the open interval (0,L) this constraint takes the form of a Volterra-type integral equation. From the definition of $\theta(t)$ it is easily seen that Equation (26) is an integro-differential inequality constraint.

The authors could not find anywhere in the literature a theorem giving conditions of optimality for a problem with such complicated constraints. To solve this problem, it was therefore necessary to develop two special theorems with the aid of the calculus of variations.

Statement of Theorems

Theorem I. For a minimum of the functional (25) it is necessary that any one of the following pairs of equations be satisfied on any part of the closed interval [0,T].

(i)
$$a < u'^*(t) < C/\theta(t) \tag{28}$$
$$Y(t) \equiv 0 \tag{29}$$

(ii)
$$u'^*(t) = a \tag{30}$$
$$Y(t) \geq 0 \tag{31}$$

(iii)
$$u'^*(t) = C/\theta(t) \tag{32}$$
$$Y(t) \leq 0 \tag{33}$$

where Y(t) is given as follows,

$$Y(t) = \theta^*_{u(t)}\Big|_{t\to T} + \int_t^T \theta^*_{u(\tau),t}\Big|_{t\to T} d\tau \tag{34}$$

Theorem II. For a strong minimum of the functional (25) it is sufficient that either one of the following pairs of equations be satisfied on the closed interval [0,T].

(iia)
$$u'^*(t) = a \tag{35}$$
$$Y(t) > 0 \tag{36}$$

(iiia)
$$u'^*(t) = C/\theta(t) \tag{37}$$
$$Y(t) < 0 \tag{38}$$

where Y(t) is given by Equation (34).

Proof of Theorems

The most general condition for the minimum of a functional is that its total variation be greater or equal to zero. If the variations are taken small the first variation will dominate all higher order terms, and a first order necessary condition for the minimum of a functional is,

$$\delta J \geq 0 \tag{39}$$

The first variation of the functional (25) can be written,

$$\delta J = \int_0^T \delta u(t)\Theta^*_{u(\tau),t}\Big|_{\substack{t\to T\\ \tau\to t}} dt + \delta u(T)\Theta^*_{u(t)}\Big|_{t\to T} + \delta Z(T)\Theta^*_{Z(t)}\Big|_{t\to T} \tag{40}$$

where $\Theta^*_{u(t)}$ and $\Theta^*_{Z(t)}$ denote standard partial derivatives of Equation (11) with Z replaced by Z(t). The quantity $\Theta^*_{u(\tau),t}$ is defined as follows,

$$\Theta^*_{u(\tau),t} = \int_0^{Z^*(t)} R^*_{1u(\tau)}\, d\xi + R^*_{2u(\tau)} \tag{41}$$

At the final time T there are two possibilities; either the maximum of Θ with respect to Z occurs on the open interval (0,L). This would imply immediately $\Theta^*_{Z(t)}\big|_{t\to T} = 0$ and the last term in Equation (40) drops out. Or the maximum occurs at Z(T) = 0 or Z(T) = L; the latter implies $\delta Z(T) = 0$ Again the last term in Equation (40) is zero. Thus δJ depends only on the variations $\delta u(t)$, $t\varepsilon[0,T]$. As the inequality (26) constrains the derivative of the function u(t) it is desired to express Equation (40) in terms of the derivative of the variation $\delta u(t)$. The variation $\delta u(t)$ and its derivative satisfy the following relationship.

$$\delta u(t) = \int_0^t \delta u'(\tau)\, d\tau \tag{42}$$

Substituting Equation (42) into Equation (40) and changing subsequently the order of integration in the first term, yields the following,

$$\delta J = \int_0^T \delta u'(t) Y(t)\, dt \tag{43}$$

where

$$Y(t) = \Theta^*_{u(t)}\Big|_{t\to T} + \int_t^T \Theta^*_{u(\tau),t}\Big|_{t\to T} d\tau \tag{44}$$

Now the conditions (i) through (iii) are easily derived. Equation (28) implies that $\delta u'(t)$ is arbitrary. Then it is easy to show[5] that we must have $\delta J = 0$ in order to satisfy Equation (39).

Applying the fundamental lemma of the calculus of variations[6] yields Equation (29). If Equation (30) defines the minimal trajectory all admissible variations $\delta u'(t)$ must be greater or equal to zero due to the constraint (26). A modification of the fundamental lemma requires then Equation (31) to be satisfied. On the other hand, $u'^*(t) = C/\theta(t)$ implies $\delta u'(t) \leq 0$ and Equation (33) follows from applying the modification of the fundamental lemma to Equation (39).

The sufficient conditions (iia) and (iiia) are obtained from the necessary conditions (ii) and (iii) by strengthening the inequality; that implies $\delta J > 0$ and as the first variation dominates all higher order terms, it implies a local minimum. It should be added that the derivative of the variation $\delta u(t)$ was not required to be small in any part of the proof. This implies that the conditions (iia) and (iiia) are sufficient conditions for a strong minimum.

Application of Sufficient Conditions

Theorem II gives immediately the solution for the equivalent problem. Implementing the lower and upper boundary control (35) and (37) numerically, shows that the sufficiency criterium $Y(t)$ is negative along the trajectory for both cases. Thus the sufficient condition (iiia) of Theorem II is satisfied whereas (iia) is not. The control law

$$u'^*(t) = C/\theta(t) \tag{45}$$

represents therefore the desired solution of the equivalent problem. As discussed previously, the same control law generates the optimal trajectory for the original minimum time problem. The minimal time t_f is found from Equation (23) with the inequality removed.

It should be mentioned that the sufficient conditions given in Theorem II are necessary and sufficient if the boundary control turns out to be optimal. If the sufficient conditions in Theorem II are not satisfied for a problem, this simply means that at least part of the optimal control must lie in the interior of the region of admissible controls. For that part of the trajectory the necessary condition (i) of Theorem I must be satisfied. Thus it is seen that the conditions of Theorem II are not always necessary.

Numerical Results

The numerical calculations are based on parameters of a typical nuclear rocket and are taken from the reference.[3] The rocket is assumed to be equipped with a graphite-uranium homogeneous reactor generating about 10^6KW in full power steady-state operation. The core is a 3 ft long x 3 ft diameter right circular cylinder with 6 inch BeO side reflectors.[7,8] The total hydrogen flow rate of the reactor is taken as 60 lbm/sec in steady-state operation. The following parameters for the fuel element are given:

Inner radius of equivalent hollow cylinder r_1 = 1/16"
Outer radius of equivalent hollow cylinder $r_2 = 2.2r_1$
Steady-state heat transfer coefficient h_o=0.77323 Btu/ft^{2}sec-^{o}R
Steady-state propellant flow rate per channel W_o=0.00433 lbm/sec
Constant of proportionality β_o = 200.9434 Btu/ft^{2}lbm-^{o}R
Equivalent half thickness of fuel element b* = 0.01 ft
Void fraction = 18.8 %
Perimeter of propellant channel $D = 2\pi r_1$ = 0.032725 ft
Specific heat of fuel element c = 0.47 Btu/lbm-^{o}R
Specific heat of hydrogen c_g = 4.1 Btu/lbm-^{o}R
Density of fuel element ρ = 101 lbm/ft^3

The steady-state power distribution is assumed to be parabolic. This is a very good approximation of the real shape in a reactor. Two cases with different curvatures are considered.

$$\text{Case I : } P_o(z)/b^* = 54000 + 9000z - 3000z^2 \text{ [Btu/ft}^3\text{-sec]} \qquad (46)$$

$$\text{Case II: } P_o(z)/b^* = 60075 + 900z - 300z^2 \text{ [Btu/ft}^3\text{-sec]} \qquad (47)$$

The latter power distribution is very flat and the reactor has therefore a somewhat higher total power generation than in case I. Both shapes of the power level were chosen to have the same maximum power generation in the center of the reactor core, and thus the same maximum thermal stress in steady-state operation. However, the maximum core temperature will be different. The transient power level is related to the steady-state level as follows,

$$P(z,\tau) = P_o(z)(1 + m\tau) \qquad (48)$$

where m takes the values -0.01, 0.0, 0.01 for the cases a, b, c respectively with $P_o(z)$ as given by Equations (46) and (47).

All calculations were done on a digital computer in the transformed variables t and Z. The input functions are in terms of the physical variables time τ and position z. The computer program converts them via Equation (4) into the transformed variables t and Z. After all computations are finished the inverse of transformation (4) is applied to give the results in terms of real time and position.

Figure 1 shows the steady-state power distributions as a function of axial position. In Figure 2 the ratio of transient to steady-state heat transfer coefficient, i.e. the physical control variable, is plotted versus time. The value of the minimum time for the six different cases can be read from the graph. It is interesting to see that the power distribution with the higher curvature permits faster flow rate (heat transfer coefficient) increases than the flatter distribution. Also, a decreasing power level leads to shorter minimum times.

From Figure 3 it is seen that the stress ratio remains on the maximum allowable limit as long as the minimum time control policy is in progress. The behavior of the stress ratio for larger times indicates that the thermal stress is roughly proportional to the power level.

The maximum core temperature as a function of time is given in Figure 4. The minimum time flow rate increase results in a comparatively fast decrease of the maximum core temperature.

Conclusions

The purpose of the paper was to find an algorithm for an increase in the propellant flow rate of a nuclear rocket in minimum time without exceeding a maximum allowable stress in the ractor core. This was achieved by deriving an analytical expression for the control law which was then implemented on a digital computer.

Core and propellant temperature of the nuclear powered rocket were described by a pair of coupled partial differential equations depending on the power generation and the propellant flow rate. The thermal stress in the core was given by a product of state and control variables. The set of partial differential equations was solved analytically in integral form for core temperature, propellant temperature and the difference between them.

The solution was then used in the formulation of the optimal control problem.

The analysis of the latter contains two significant steps. 1. It is shown how the minimum time problem can be reformulated in terms of an equivalent minimum cost index problem where this cost index is written for a fixed final time. A minimization problem with a fixed final time is in general more easily solved than a minimum time problem. The authors believe that the conversion technique demonstrated in this paper is general enough to be applicable in other cases. 2. In order to solve the engineering problem two theorems had to be derived giving necessary and some sufficient conditions for the minimum of a functional subject to certain integro-differential constraints. These theorems apply only to the particular problem of this paper and are based on the application of unilateral variations. The importance of this analysis lies in the fact that sufficient conditions for a strong minimum were derived by applying only basic principles of the calculus of variations. This demonstrates that very complex problems can sometimes be solved with very simple means.

The sufficiency conditions of Theorem II have been used to establish that upper boundary control gives a strong minimum for the equivalent problem. The control law is in feedback form and represents the minimum time control policy.

The numerical results obtained give a good feeling for the dynamic response of the nuclear rocket engine. A power distribution with a higher curvature permits faster increases in the propellant flow rate and a decreasing power level has a similar effect.

References

1. Wittler, M., Optimal Nuclear Rocket Control Subject to Integro-Differential Constraints, Doctoral Thesis, Rensselaer Polytechnic Institute, June 1968, p. 19.
2. Briggs, D. L. and C. N. Shen, Switching Analysis for Constrained Bilinear Distributed Parameter Systems with Applications, presented at the Joint Automatic Control Conference at the University of Michigan, Ann Arbor, June 1968, and to be published in the Transactions of the ASME.

3. Shen, C. N. and T. C. Liu, Transient Heat Transfer and Thermal Stress for a Nuclear Rocket due to Sudden Increase of Coolant Flow, ASME paper No. 66-WA/NE-4, 1966.
4. Kreith, F., Principles of Heat Transfer, International Textbook Company, 1960, p.345.
5. Gelfand, I. M. and S. V. Fomin, Calculus of Variations, Prentice-Hall, 1963, p. 13.
6. Ibid., p. 9.
7. Hanson, G. E. et al., Beryllium-Reflected, Graphite-Moderated Critical Assemblies, AEC Report LA-2141, 1957.
8. Ragsdale, R. G. and F. E. Rom, Advanced Concepts for Nuclear Rocket Propulsion, NASA Sp-20, 1962.

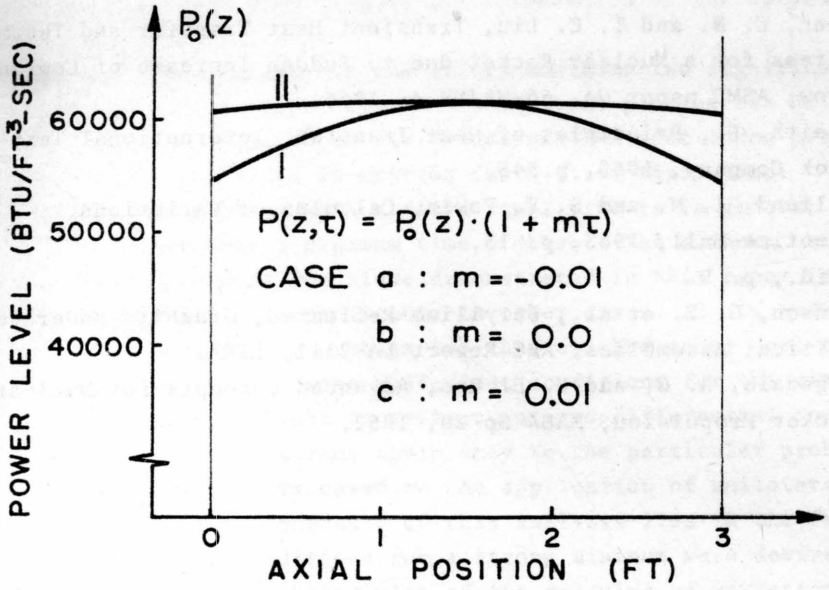

FIGURE 1 STEADY-STATE POWER LEVEL AS A FUNCTION OF AXIAL POSITION

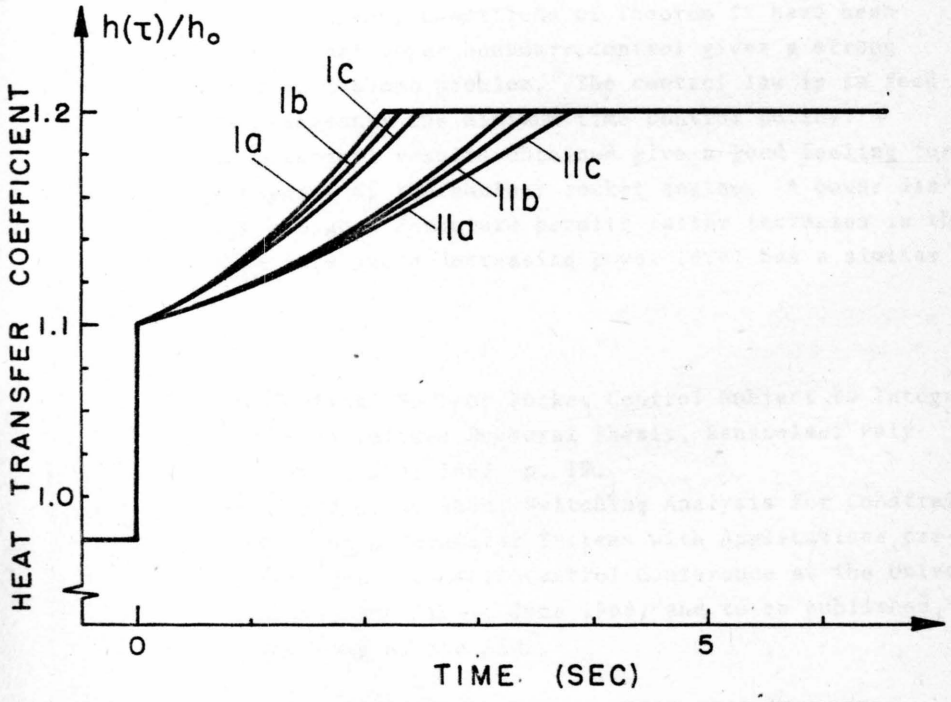

FIGURE 2 RATIO OF TRANSIENT TO STEADY-STATE HEAT TRANSFER COEFFICIENT VERSUS TIME

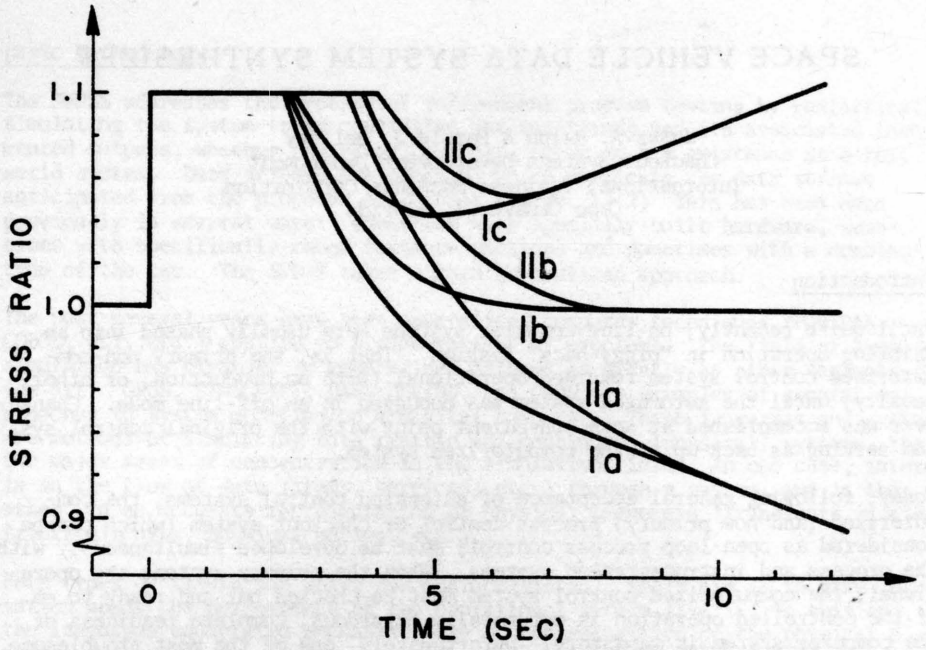

FIGURE 3 RATIO OF MAXIMUM TRANSIENT TO STEADY-STATE THERMAL STRESS VERSUS TIME

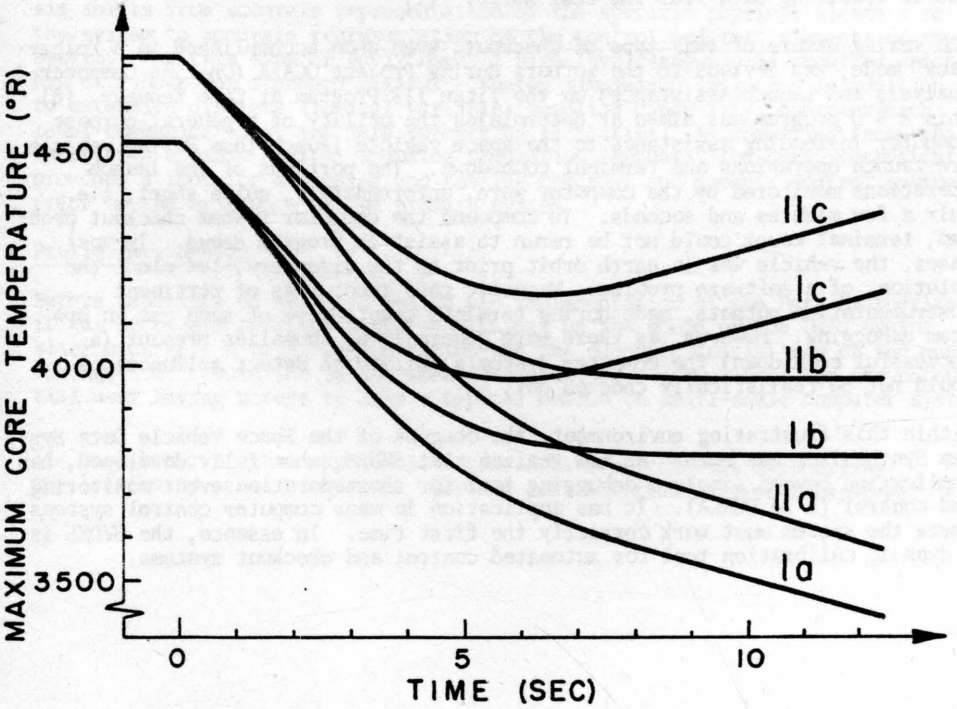

FIGURE 4 MAXIMUM CORE TEMPERATURE VERSUS TIME

SPACE VEHICLE DATA SYSTEM SYNTHESIZER

James A. Ralph & Harold J. Bellamy
Checkout Systems Development Department
International Business Machines Corporation
Cape Canaveral, Florida

Introduction

Until quite recently, on-line computer systems were usually phased into an existing operation in "piggy-back" fashion. That is, the primary non-computerized control system remained operational (with no production, or other, penalty) until the automated system was debugged in an off-line mode. Change-over was accomplished at some convenient point with the original control system serving as back-up to the computerized system.

Today, following general acceptance of automated control systems, the computerized (and now primary) process control or checkout system (which can be considered as open-loop process control) must be developed simultaneously with the process and instrumentation systems. When the primary systems are operational, the computerized control system must be checked out and ready to go. If the controlled operation is potentially hazardous, complete readiness of the computer system is mandatory. Unfortunately, one of the most troublesome aspects of any on-line computer system is checkout. It is nearly impossible to give the system a comprehensive check until it has been installed on-line and is receiving data from the real world. (1)

The vexing nature of this type of checkout, even when accomplished in a "piggy-back" mode, was obvious to the authors during Project OCALA (On-line Computer Analysis and Launch Assistance) on the Titan III Program at Cape Kennedy. (6) This R & D program was aimed at determining the utility of a general-purpose computer in lending assistance to the space vehicle launch team during vehicle pre-launch operations and terminal countdown. The portions of the launch operations monitored by the computer were, unfortunately, quite short, i.e., only a few minutes and seconds. To compound the computer system checkout problem, terminal count could not be rerun to assist in program debug. In most cases, the vehicle was in earth orbit prior to the discovery, let alone the solution, of a software problem. Magnetic tape recordings of pertinent instrumentation outputs, made during terminal count, were of some use in program debugging. However, as there were generally no anomalies present (a successful countdown) the computer system's ability to detect malfunctions could not be realistically checked out.

Within this frustrating environment, the concept of the Space Vehicle Data System Synthesizer was born. We now realize that SVDSS, when fully developed, has application beyond simply a debugging tool for short-duration event monitoring and control (a la OCALA). It has application in many computer control systems where the system must work correctly the first time. In essence, the SVDSS is a dynamic calibration tool for automated control and checkout systems.

Basic Methodology

The SVDSS addresses the problem of independent program testing by realistically simulating the system to be controlled (or monitored) and its associated instrumented outputs, whether analog or discreet, prior to its existence as a real-world system. Data streams are produced which duplicate the data streams anticipated from the proposed functional system. (1,2) This has been done previously in several ways: sometimes with specially-built hardware, sometimes with specifically-coded software packages and sometimes with a combination of the two. The SVDSS takes a more generalized approach.

The past several years have seen generalized computer techniques (FORTRAN, COBOL, PL1, etc.) applied to a wide variety of problems. The field of computer simulation has expanded in generalized methods as greatly as other segments of the art. GPSS, SIMSCRIPT, DAS, DSL/90, and CSMP are examples of general approaches to system modeling on a digital computer. These languages and systems are methods of simulating both traffic and continuous (physical) systems, the two major areas of concentration in the simulation field. In one case, interest is in the flow of data (items, services, etc.) through a system, and in the other, in an accurate representation of physical phenomena (transients in electrical circuits, physical motion, etc.).

Both types of simulation share one characteristic: their aim is to give information about the performance of the operational system itself. To this end, the languages enumerated emphasize ease of representation of the physical elements of the system.

When considering a system in a checkout or process control environment, emphasis shifts from accurate representation of the specific physical elements of the system to accurate representation of the control and test elements of the system. For this type of environment a high-level language is required which has attributes of standard digital - analog simulation languages in addition to extensive discrete (logical variable) handling capability, operator/math model communications, and data formatting facilities. By combining these features with a basic digital - analog simulation language, the Data Synthesizer provides a tool for designing and testing checkout and process control systems prior to the existence of the primary system.

Preliminary Design

Before embarking on detailed design and implementation of the Data Synthesizer, it was necessary to place basic constraints on the scope of the Data Synthesizer package. A prime consideration was the economic feasibility of the undertaking, i.e., could the SVDSS, when developed, be a useful tool for the potential user having access to only a typical medium to small-scale computer system?

The most basic of these system size considerations concerns synthesizer-applications program residence. Several possibilities suggest themselves:

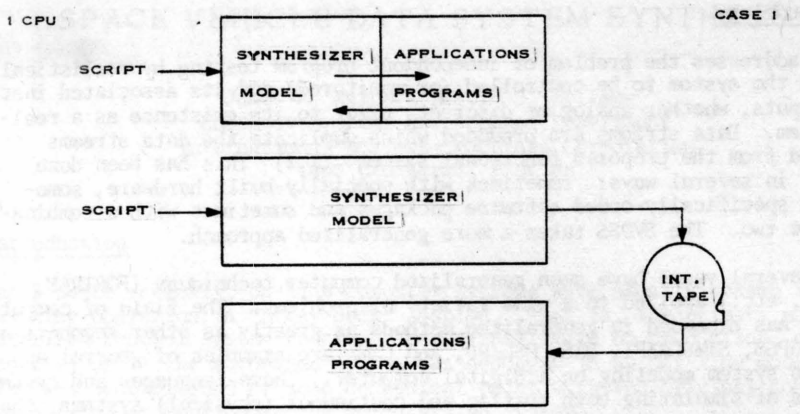

When a single CPU is available, two cases should be considered. In the first case, both the synthesizer and applications programs reside in main storage concurrently. The synthesizer model runs, accepts inputs from script language and applications programs, and provides data to the applications programs. Aside from the problem of the interface between the synthesizer model and the applications programs, the major constraint is the amount of core storage necessary to contain both the model and the applications programs. It is probable that concurrent residence would require a main store of such size that the system could be run only on the largest of computer systems. The alternate approach, using a single CPU, is to run the model with script inputs, produce a formatted output tape, and run this tape against the applications programs to be tested. Here, the core storage requirements are much lower than with concurrent residence, but the system loses the ability to simulate an active system. The applications programs can react to data from the model but they cannot interact with the model to change the characteristics of the data flow. The trade-off between simulation capability and computer system size is again evident when more than one CPU is considered.

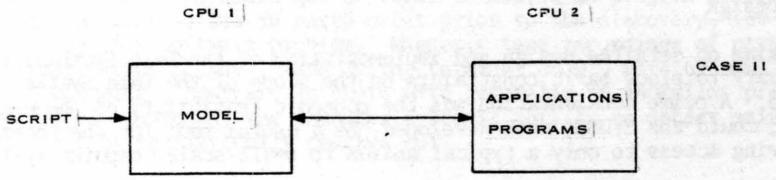

This type of arrangement has all the advantages as the concurrent residence system and is easier to program, since the multi-programming required in the single CPU system has been largely eliminated.

Neither of the second alternatives (use of an intermediate tape or multiple CPU's) is acceptable; the first because of its inability to represent active systems and the second because multiple CPU configurations are seldom available. The alternative of concurrent residence of mathematical model and applications' programs in the same main storage became the only possibility. Our IBM/Cape Kennedy facility computer - an IBM System 360/40 with 128K bytes of main storage - is a typical medium-to small-scale system. The decision was made to go ahead with implementation and, should the computer system prove too small, re-evaluate the economic feasibility of the project.

In addition to the problem of the size of the processor needed to run the Data Synthesizer, there was one other segment which required apparently arbitrary constraints. This was the section of the mathamatical model - interface - checkout program complex which deals with the hardware system data interface. There is no standard computer interface. Characteristics vary in such critical areas as buffer size, conversion capabilities, and interrupt structure, to name a few. It did not appear possible to provide a high-level language that was specific enough to be used to describe the logic of the computer interface. Furthermore, the time required (even with a special language) to produce a model of an interface would be prohibitive for the return derived. Therefore, it was decided that the interface model would consist of a data formatter (with appropriate language facilities) and would include interface characteristics beyond data format only to the extent that allowable execution time for the checkout programs was effected.

System Description:

It is best to describe the Data Synthesizer system by summarizing the functions of a checkout program and the conditions under which it operates, then to match them with related sections of the Data Synthesizer system.

In the simplest view, a checkout or control program accepts data from a functional system, performs certain calculations and manipulations, and then takes action based upon the results it has obtained. The rate at which input data is presented to the checkout program determines allowable execution time for the checkout program.

The action taken by the program may be to put command signals into the functional system (active), or it may be to log results or display them so that appropriate action may be taken by the operator (passive). Of these operations, the Data Synthesizer system is concerned with all but the calculations done by the checkout program. Therefore, the Synthesizer must: 1) provide a method for producing a mathematical model which can be controlled by inputs from the operator and/or feedback from the checkout program; 2) format parameter (discrete and analog) data which has been produced by the mathematical model and 3) control the execution of the checkout program in a manner analogous to the control exercised by a hardware interface. The Synthesizer system can then be considered in two major sections: a mathematical modeling section which provides facilities for easy description of the physical system to be simulated, and a data format/execution control section which formats data for the applications programs and provides execution control for both the mathematical model and the applications (checkout) programs. The mathematical modeling section is based upon the Continuous System Modeling

Program (CSMP) developed for the IBM System/360. CSMP/360 was chosen because its modularity and base language (FORTRAN) make it easy to modify. CSMP/360 is a typical analog-digital simulation language which provides a selection of integration routines, a number of special functions, execution control and specialized output routines. In its unmodified form, it is not directly useable in the Data Synthesizer because of the following restrictions:

- Logical variable facilities are limited to two input AND and OR gates with a full 32-bit word of storage used to represent each variable. Since most launch vehicle systems include extensive logic control, this limited capability for logic modeling would be prohibitively slow and wasteful of core storage.

- Operator control of mathematical model execution is not possible with CSMP/360. In both launch vehicle checkout and process control applications, the man-in-the-loop is important enough to make easy operator-model communications a necessity.

Execution Control and Data Formatting:

Launch Vehicle checkout systems are oriented heavily toward time-based events and logical control. A simulation program for the Apollo Spacecraft Emergency Detection System developed at Cape Kennedy employs a unique algorithm for simulation of purely discrete systems. (5) The algorithm is based on a control matrix and associated tables. The matrix is scanned during each computation cycle to determine state changes in any of the system discretes. Occurrence of a particular discrete signal triggers all associated discretes and these are passed, when required, to the checkout program which, in turn, can set discretes in the control matrix.

Generation of the control matrix requires that the logic system, to be simulated, be described in terms of Boolean logic. Inherent in such a description is the ability to include logic equations with time as one of the variables, thus including a time-based sequence of events or script.

Since communication between the controlling computer system and the functional system is usually through discrete signals, and the control matrix algorithm is known to be a fast and effective method for simulating discrete systems, it was natural to incorporate the control matrix into the Data Synthesizer System.

Figure 1 illustrates the interaction, during execution, of the different modules of the Data Synthesizer.

Systems Inputs

Inputs to the Data Synthesizer can be divided, for discussion purposes, into three types: standard CSMP/360 statements, Boolean equations, and typewriter inputs. Figure 2 shows examples of each type of input. Since CSMP/360 statements are described in detail in other publications (IBM manual H20-0367-2), discussion here will be confined to Boolean equations and typewriter inputs.

The Boolean translator is the main addition made to CSMP/360 and performs several functions. These functions are: reduction of symbols from up to fifteen characters to six characters where required, collection of terms, sorting of terms, generation of a list of MACRO statements for input to the OS/360 assembler and, finally, production of a list of variables for display and typewriter communication.

When the Boolean equations which describe the logic of a system to be synthesized are derived, it would be advantageous to retain the same nomenclature used in the system schematics. However, the FORTRAN compiler restricts the user to six characters per variable name and, by extension, so does CSMP/360. To increase ease of use, the Boolean translator will accept parameter names up to fifteen characters in length and, where necessary, will generate internal names of six or less characters in length.

Ease of use is also increased by providing a sorting process similar to that of CSMP/360. The user need not order his equations so that all elements are evaluated before any equation is encountered. The sorting process accomplishes this and the user need only be sure that his equations are adequate to describe the system.

After generating any internal names required and performing the sort, the translator produces a list of MACRO's which reflect the logical functions described in the equations. These MACRO's are then input to the OS/360 Assembler and the output is the control matrix previously described. At the time the equations are being reduced and the MACRO's generated, lists of variables are prepared for display on the high-speed printer or for reference from the console typewriter. Variables are defined in the tables by name vs. matrix location. Typewriter inputs are made while the model is being run on the computer. Requests are made by typing an appropriate verb and a variable designation at the console and entering this message into the computer. A limited set of verbs are available to the operator. The number can readily be expanded as the needs are defined. The available verbs and their functions are:

VERB	VARIABLE NAME	
ON	XXXXXX	Turn designated discrete signal "ON" by setting to 1.
OFF	XXXXXX	Turn designated discrete signal "OFF" by setting to 0.
INV	XXXXXX	Invert designated discrete signal if 1 set to 0, if 0 set to 1.
SET	XXXXXX	Applies to analog values only. Designated value is set by next message after computer requests typewriter input.
STATUS		Request printout of status of all variables. This printout is done on high-speed printer.

Application Description

In the course of developing the Data Synthesizer, a demonstration of its utility was required. The criteria used in selecting a test application can also serve as a guide to potential Data Synthesizer applications. Wherever a significant number of the conditions enumerated here exist, the Data Synthesizer will probably prove to be a useful study of system development tool.

- The demonstration system should consist of both continuous physical elements and discrete logic control and test elements
- The demonstration system should be self-contained, at least to the extent that any outside phenomena which affect the system are readily approximated.
- The hardware to be studied need not exist but if it does exist, is not available for developmental purposes.
- Development of some form of digital computer monitoring or control is desired.

Finally, it was preferable that the first application of the Data Synthesizer yield useful results and be more than an academic exercise.

The method of selecting a system for study and the approach used is described in detail because most of the problems encountered and decisions taken are typical of checkout or process control investigation in general.

The system chosen was the non-cryogenic (RP-1) propellant loading system for the Saturn launch vehicle at Cape Kennedy.

RP-1, liquid hydrogen (LH^2), and liquid oxygen (LOX) are loaded into the Saturn L/V by three separate systems. The three systems are similar except that the LOX and LH^2 systems are much more complex than the RP-1 system.

There is considerable interest in using a digital computer to increase the degree of automation of the loading process, and particularly in the ability of the loading system to react to malfunctions. Ideally, should a malfunction occur during propellant loading, a highly-automated system would attempt to take corrective action and, if this were impossible, inform the operator of the precise nature of the malfunction so that corrective action could be taken immediately. While it seems evident that such a system is possible, it is necessary to demonstrate that it is. Beyond demonstrating that a fully automated system is theoretically possible, it is also desirable to learn the type of control which would give these results and the practical level of automation which can be achieved.

Since the three systems are similar, the most practical approach to the problem is to study the RP-1 system because it is the simplest of the three. If useful results can be obtained, similar results for the LOX and LH^2 systems would require only an extension in complexity of the same basic approach taken for the RP-1 loading system.

Figure 3 is a simplified block diagram of the RP-1 system. The areas enclosed by dashed lines represent the functional divisions of the system. Section I includes only the control panels in the Launch Control Center (LCC). These panels are equipped with pairs of colored lights which indicate the state of each valve in the system, and control switches for each valve. In normal procedure, the operator sets a switch to put the system in automatic and depresses the "Fill" button after which fueling is automatic. In the event of malfunctions or other unforeseen events, the fueling process can be controlled manually from the control panels using panel switches to operate the appropriate valves.

Section II includes the Propellant Tanking Computer System (PTCS) and the relay control logic. The PTCS acts mainly as a sequencer which monitors the level of liquid in the tanks and issues mode change (i.e., start fast fill, stop fast fill) commands to the relay system based on tank liquid levels.

In the event of a malfunction, such as a mispositioned valve, the fueling system undergoes "reversion" to a safe condition and an indication of this action is displayed on the Launch Control Center (LCC) control panels. Detection of the mispositioned valve and subsequent system reversion are controlled by the Relay Control System. When the system undergoes reversion, all the valve position changes (this may include most of the valves being used) are displayed on the LCC panels. Since reversion takes a very short time, the operator at the control panel can detect only that a malfunction has occurred and that the system has reverted. Subsequent malfunction isolation is made more troublesome by the fact that all recording devices will show the action taken during reversion as well as those which lead up to the malfunction.

Section III includes the tanks, pipes and valves which comprise the fuel transfer system.

If we now compare the RP-1 fueling system in its logical division (Figure 3) we can correlate each section of the actual system with the corresponding part of the Data Synthesizer (Figure 1). In so doing, we can also demonstrate a useful feature of the Data Synthesizer. Note that Section I of Fueling System corresponds to the operator requests block in Figure 1, Section II corresponds to the control matrix and Section III to the Continuous phenomena integration and update routines.

Before carrying this analogy further it is necessary to refer to the original statement of the problem and to consider how a digital computer might be added to the system. The two most obvious courses are to add a passive digital computer to the fueling system (which would remain intact) and to replace the existing relay control system with an active digital computer. Two possibilities would be approached using the Data Synthesizer:

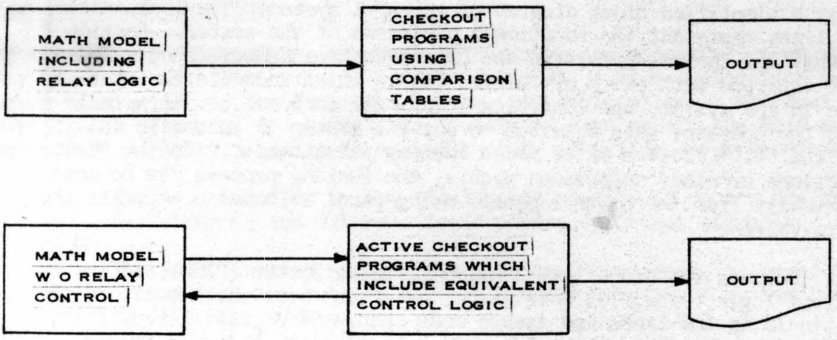

Regardless of which type of system is to be studied, a detailed analysis of the relay control logic is necessary. Once the control logic has been reduced to Boolean equation form, it can be translated by the Data Synthesizer either into the control matrix for the mathematical model or into an additional matrix which is executed as a part of the checkout program.

In the case being discussed, primary interest is in the development of algorithms to isolate malfunctions. Therefore, the relay control logic was incorporated into the mathematical model and the checkout programs receive discrete data specifying valve positions and the state of the liquid sensors in the fuel lines. Mass readout and flow rates as well as differential pressure across fuel filters are presented as analog data. Execution time for the checkout programs is arbitrary since a data interface has not been specified. The relative slowness of the fueling process permits considerable freedom in execution time and 200 ms was chosen as the execution interval for the applications programs.

Application Summary

The steps in applying the Data Synthesizer to the RP-1 system are typical of those required for its use with any system. They are:

- Systems selection - determine whether the system is of a type emenable to SVDSS analysis.
- System definition - isolate the system to be studied (if necessary) and identify any constraints of system modeling.
- System analysis - derive all equations necessary to describe continuous and discrete phenomena in the system.
- Interface definition - define the characteristics of the data interface.

When these steps have been accomplished, and inputs to the Data Synthesizer prepared, the checkout programs and the model can be loaded together and the task of checkout program development and debug begun. In the particular application discussed here, it was found that in the process of modeling the physical system a good deal of the analysis done was directly applicable to the development of the required control programs.

Potential Data Synthesizer Applications

Once the concept of the data Synthesizer System has been accepted a number of potential applications can be identified.

The parallel between launch vehicle checkout and commercial process control is evident. Here the process (chemical, petroleum transport piping, etc.) is modeled using the continuous model part of the system and the applications programs represent the functions carried out in the on-line computer.

Wherever there is interaction, either active or passive, between digital computer and some process which is continuous in nature, the Data Systems Synthesizer may be useful.

Sometimes the data generation (passive) mode of usage can be used in applications which are not so obvious. Given a piece of hardware designed to handle a multitude of inputs which are changed by means of something like a patch panel it is possible to replace the hardware normally connected to such a device with a digital computer. The Data Synthesizer provides a quick and convenient means for programming the digital computer to provide realistic data to the device in question without requiring the presence of the actual hardware. Such an application is being considered at IBM Cape Kennedy in connection with a training device which is a replica of the control panels used to conduct launch vehicle checkout. After connection of this device to a digital computer the Data Synthesizer can be used to generate data which is characteristic of the different systems to be monitored by the control panels. All that is required to change from one system to another is to bring a different SVDSS model into the computer.

A most intriguing possibility for Data Synthesizer usage is in biomedical research. There is much interest in using digital computers for patient monitoring. However, there is reluctance to entrust a live human being to the care of a computer, so investigation in this area is difficult.

This situation is typical of problems noted earlier as fertile ground for Data Synthesizer applications: i.e.: the need to develop techniques exists but direct application of the computer for study purposes is troublesome or impossible. The major unanswered question is: can the physiological system to be studied be defined, and, having been defined, can it be modeled? There has been considerable work in the field of mathematical modeling of physiological systems. (3,4) Mainly modeling has been used to study the mechanism of the physiologic system itself. Certainly it is theoretically possible to apply the Data Synthesizer to patient monitoring. Whether it can or not is dependent on the state of the art in physiological modeling.

Earth resources control and investigation is one of the most recently opened fields for digital computer applications. Flood control, water distribution and petroleum transport systems can be included in this category, as well as air pollution monitoring systems.

Typically, such systems consist of a network of remote terminals which collect and transmit data to a central computer. The computer, in turn, can correlate the data received and, if required, transmit signals back to the remote terminals for flood gate control or other action appropriate to the system in question. Naturally, the applicability of the Data Synthesizer depends on the nature of the system function. Simulation of air flow (for air pollution monitoring) is very difficult even when only a reasonable approximation is required. On the other hand, water distribution systems should be amenable to simulation, and so provide candidate systems for Data Synthesizer use.

Because of the complicated interaction between the central computer and the remote terminals, it would be necessary to provide programs beyond those normally required in Data Synthesizer applications; but considerable time still would be saved over a "cold start" approach to an earth resources system.

In summary, the Space Vehicle Data System Synthesizer, a software system initially conceived for and applied to space vehicle systems, has potential application in other areas of scientific endeavor. Earth resources and physiological sensing system output simulation are but two. Other areas are being explored.

References

1. Memorandum RM-4161-NASA Vol. II
   The Rand Corporation, July 1964

2. MUSE (Multi-User Environment Simulator)
   E. W. Pullen, D. F. Shuttee
   Proceedings AFIPS Vol. 32 1968 S.J.C.C.

3. "Study of Mamalian Adrenal Glucocorticoid System by Computer Simulation"
   F. E. Yates, ?R. D. Brennan
   IBM Technical Report No. 320-3228

4. "Simulation of Physiological Mechanisms"
   A. C. Guyton, H. T. Milhorn, Jr., and T. G. Coleman
   Proceedings of IBM Computing Symposium on Digital Simulation of Continuous Systems

5. "Computer Simulation of Complex Boolean Expressions"
   R. L. Chew III, A. D. Hearn
   New Technology Report S14000-004

6. "Project OCALA"
   L. B. Perkins, J. A. Ralph
   Instrument Society of America Symposium, 1966
   Cocoa Beach, Florida

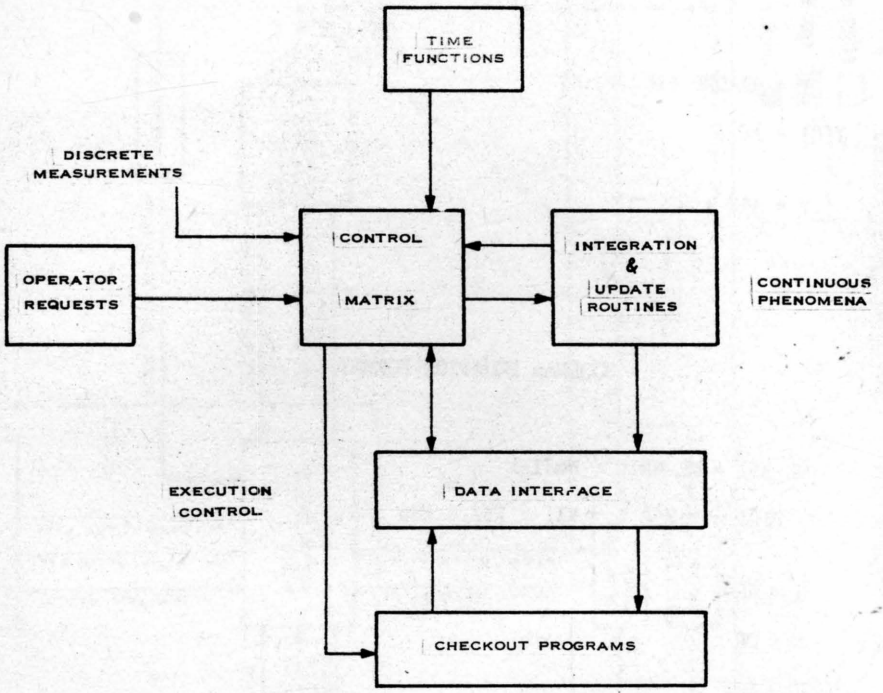

Figure 1. Basic Execution Logic For Data System Synthesizer

TYPICAL CSMP/360 STATEMENTS

```
   Y = INTGRL (IC, X)                    Y = ∫_0^t Xdt + IC
Y(0) = IC

                                         PẎ + Y = X

   Y = REALPL (IC, P, X)
Y(0) = IC

   Y = A*X + B
```

BOOLEAN EQUATION FORMAT

```
  ML-K91 = ML-6DIR & W6J1-1
    P101 = ¬K50 & ¬K51 + K52 & K86

  & = AND
  + = OR
  ¬ = NOT
```

Figure 2

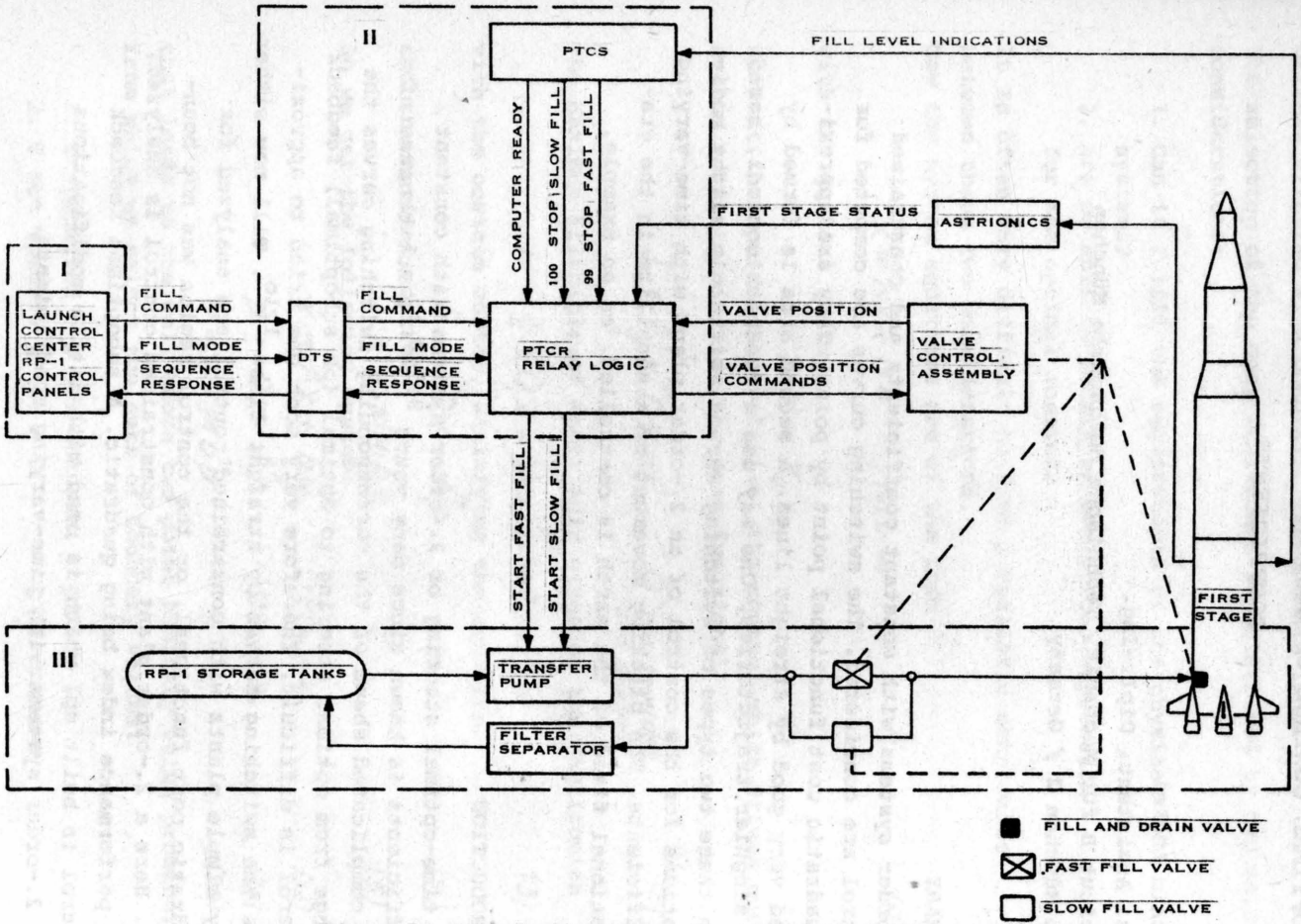

Figure 3. RP-1 Fueling System Simplified Block Diagram

SUBOPTIMAL CONTROL OF 2. ORDER PLANTS WITH TIME-VARYING COEFFICIENTS

Joachim Lückel
Wiss. Assistent, Dipl.-Ing.
Institut B für Mechanik, Technische Hochschule München
8ooo München 2 / Germany

SUMMARY

2.-order systems with constant coefficients and constrained control are considered. The switching curves are computed for a quadratic cost functional point by point. They are approximated very good by straight lines. A second area is formed by the singular trajectories. One may use a feedback control, based upon these two types of switching curves, with only slight modifications for the control of an 2.-order plant with time-varying coefficients. The pitching movement of a satellite in the gravitational field of the earth is controlled, as an example.

INTRODUCTION

The time-optimal steering of 2.-order systems with constant coefficients is known since many years [9,5,2,1]. But because of the complicated shape of the corresponding switching curves the change from optimal steering to optimal (or suboptimal) feedback control is difficult. Therefore very soon one tried to approximate the switching curves by straight lines [1,1o]. Till now either only simple plants with constrained control are analyzed for quadratic cost functional, or the control region was not bounded. Here a 2.-order plant with constrained control is analyzed, the performance index being quadratic. A suboptimal feedback control is built up, which is used with little modifications for 2.-order systems with time-varying coefficients.

OPTIMAL STEERING WITH QUADRATIC PERFORMANCE INDEX

The selection of the cost functional is determined by two main considerations:

1. Can it fulfil the requirements of the physical systems?
2. Are we able to obtain an analytical expression for the optimal control?

It is often very difficult to find a realistic compromise between these two considerations.
Now the system equations are of the form

$$\dot{x} = Ax + bu \qquad |u| \leq u_0 \tag{1}$$

with the initial state

$$x(t_0) = x_0$$

We want the optimal control, i.e. the control which drives our system so as to minimize the cost functional

$$J = \tfrac{1}{2}\int_0^T x^T Q x \, dt \qquad Q \text{ pos. semidef. and symm.} \tag{2}$$

The Maximum-Principle of Pontrjagin gives us the Hamiltonian

$$H = \tfrac{1}{2} x^T Q x + (Ax)^T p + (bu)^T p \tag{3}$$

with the costate vector, satisfying the equation:

$$\dot{p} = -Qx - A^T p \tag{4}$$

and the optimal control

$$u = u_0 \, \text{sign}\, b^T p \tag{5}$$

So we get the following system:

$$\dot{x} = Ax + bu \qquad x(t_0) = x_0 \tag{1a}$$

$$\dot{p} = -Qx - A^T p \qquad p(t_0) = p_0 \tag{2a}$$

$$u = u_0 \, \text{sign}\, b^T p \tag{3a}$$

that leads to the well known two point boundary value problem, from which we select two sets of boundary values:

1. T specified x (T) unknown, $p(T) = 0$
2. T not specif. x (T) = 0 p(T) unknown

There is no analytical solution for the systems.

2.-ORDER PLANT WITH CONSTANT COEFFICIENTS

First we will analyze the 2.-order plant with constant coefficients:

$$\begin{bmatrix} \dot{x}_1 \\ \dot{x}_2 \end{bmatrix} = \begin{bmatrix} 0 & 1 \\ -b & -a \end{bmatrix} \begin{bmatrix} x_1 \\ x_2 \end{bmatrix} + \begin{bmatrix} 0 \\ 1 \end{bmatrix} u \qquad \begin{matrix} x_1(t_0) = x_{10} \\ x_2(t_0) = x_{20} \\ |u| \leq u_0 \end{matrix} \tag{6}$$

$$J = \tfrac{1}{2} \int_0^T x^T Q x \, dt; \qquad Q = \begin{bmatrix} A & 0 \\ 0 & B \end{bmatrix} \tag{7}$$

The system is controllable and normal.

We have the costate system:

$$\begin{bmatrix} \dot{p}_1 \\ \dot{p}_2 \end{bmatrix} = \begin{bmatrix} A x_1 \\ B x_2 \end{bmatrix} - \begin{bmatrix} -b p_2 \\ p_1 - a p_2 \end{bmatrix} \qquad p_2 = -1 \tag{8}$$

and the optimal control (of the Bang-Bang type):

$$u = u_0 \, sign \, b^T p = u_0 \, sign \, p_2 \tag{9}$$

There also exists no analytical solution for this simplified system. But it is possible to solve the above system backward in time and find out points of the switching curve in the phase plane.

With $\phi = T - t$ we obtain $d/d\phi = -d/dt$ and:

$$x' = -Ax - bu \qquad x(\phi=0) = \bar{x}_0 \tag{6a}$$

$$p' = Qx + A^T p \qquad p(\phi=0) = \bar{p}_0 \tag{8a}$$

$$u = u_0 \, sign \, p_2 \qquad ' = d/d\phi \tag{9a}$$

1. T specified $x(T) = \bar{x}(0)$ unknown

It can be shown, that one portion of the x_1-axis itself is part of the switching curve. Therefore we begin with:

$$\bar{x}_{10} = \pm \eta \, ; \; \bar{x}_{20} = 0$$

The analogue computer is a very good tool for the initial computation. Yet the construction of the whole switching curve is a very time consuming task. Therefore it is better to try the automatic solution on a digital computer. We break up the whole trajectory into parts, such that the final state of each part lies on the x_1-axis. Now we are able to compute easily the switching curve for these parts.

a) $b > a^2/4$ (oscillating motion)

With the initial state $\bar{x}_{10} = \eta$; $\bar{x}_{20} = 0$;

$u = \pm u_0$ we obtain the solution

$$x_1 = -\frac{a}{2\Gamma} e^{a/2\phi} \sin\Gamma\phi \left(\eta \mp \frac{u_0}{b}\right) + e^{a/2\phi} \cos\Gamma\phi \left(\eta \mp \frac{u_0}{b}\right) \pm \frac{u_0}{b} \tag{10}$$

$$x_2 = \frac{b}{\Gamma} e^{a/2\phi} \sin\Gamma\phi \left(\eta \mp \frac{u_0}{b}\right) \tag{11}$$

$$b/A\, p_2 = \left[\cos\Gamma\phi \left(e^{-a/2\phi} - e^{a/2\phi}\right) + \frac{a}{2\Gamma} \sin\Gamma\phi \left(e^{-a/2\phi} + e^{a/2\phi}\right) + \frac{F}{\Gamma} \sin\Gamma\phi \left(e^{-a/2\phi} - e^{a/2\phi}\right)\right] \eta$$

$$\pm \frac{u_0}{b} \left[\cos\Gamma\phi \left(e^{-a/2\phi} + e^{a/2\phi}\right) + \frac{a}{2\Gamma} \sin\Gamma\phi \left(e^{-a/2\phi} - e^{a/2\phi}\right) - \frac{F}{\Gamma} \sin\Gamma\phi \left(e^{-a/2\phi} - e^{a/2\phi}\right) - 2\right] \tag{12}$$

$$\Gamma = \sqrt{b - a^2/4}\,; \quad F = b/a\,(1 + bB/A) \tag{13}$$

We eliminate η from (10) and (11) and with $p_2 = 0$ we find points of the switching curve for all $0 < \phi < \phi_{lim.}$.

$$x_{2sw} = \mp \frac{u_0}{b} \frac{e^{-a/2\phi}\left(2\cos\Gamma\phi + \frac{a}{\Gamma}\sin\Gamma\phi\right) - 2}{e^{-a\phi}\left(\frac{\Gamma}{b}\cot\Gamma\phi + \frac{a}{2b} + \frac{F}{b}\right) - \frac{\Gamma}{b}\cot\Gamma\phi + \frac{a}{2b} - \frac{F}{b}} \tag{14}$$

$$x_{1sw} = \frac{x_{2sw}}{b}\left(\Gamma\cot\Gamma\phi - a/2\right) \pm \frac{u_0}{b} \tag{15}$$

b) $a^2/4 > b$ (aperiodic motion)

Only one switching is used:

$$x_{2sw} = \mp \frac{u_0}{2\Gamma} \frac{\left[(B_1 + B_4)e^{a_2\phi} + (B_2 + B_3)e^{-a_1\phi} - 4\Gamma A_1\right](e^{a_1\phi} - e^{-a_2\phi})}{B_1 e^{a_2\phi} + B_2 e^{-a_1\phi} - B_3 e^{a_1\phi} - B_4 e^{-a_2\phi}} \tag{16}$$

$$x_{1sw} = \frac{x_{2sw}}{b}\left(\frac{a_1 e^{a_1\phi} + a_2 e^{-a_2\phi}}{e^{a_1\phi} - e^{-a_2\phi}} - a\right) \pm \frac{u_0}{b} \tag{17}$$

$$A_1 = A/b\,; \quad A_2 = \frac{A(a^2+b) + b^2 B}{ab}\,; \quad A_3 = \frac{A(a^2-b) - b^2 B}{ab}$$

$$\Gamma = \sqrt{a^2/4 - b}\,; \quad a_1 = a/2 + \Gamma\,; \quad a_2 = -a/2 + \Gamma$$

$$B_1 = A_1 a_2 + A_2\,; \quad B_2 = A_1 a_1 - A_2$$

$$B_3 = A_1 a_1 - A_3\,; \quad B_4 = A_1 a_2 + A_3 \tag{18}$$

For given ϕ the switching curves can be easily computed for both types of motion by a digital computer.

2. T not specified $X(T)=\bar{X}(0)=0$

Here we do not know the initial state of the costate system. If we select

$$\bar{p}_{10} = \cos\psi \quad \bar{p}_{20} = \sin\psi \qquad 0<\psi<\pi \tag{19}$$

we find points of the switching curve on an analogue computer.

EXTREMAL SINGULAR CONTROL

The switching function $b^T p$ being zero for one ore more positive interval of time, we obtain no necessary conditions for the optimal control and we speak of singular trajectories.

Yet if we find an extremal control (i.e. a control which obeys the conditions of the maximum principle) with the property: $b^T p = 0$ in a positive interval of time, we get an extremal singular control.[1,3,6]

Therefore the condition for a singular trajectory is given by:

$$b^T p = 0 \qquad t \in (t_1, t_2) \tag{20}$$

In our problem

$$p_2(t) = 0; \quad t \in (t_1, t_2) \qquad \dot{p}_2(t) = 0 \tag{21}$$

and with the singular control holds:

$$u = (1+b)x_1 + a x_2 \tag{22}$$

This implies in our system:

$$\begin{aligned} \dot{x}_1 &= x_2 \quad ; \quad x_{10} = \xi_1 \\ \dot{x}_2 &= x_1 \quad ; \quad x_{20} = \xi_2 \end{aligned} \tag{23}$$

with the solution:

$$x_1 = \tfrac{1}{2} e^{t}(\xi_1 + \xi_2) + \tfrac{1}{2} e^{-t}(\xi_1 - \xi_2) \tag{24}$$

$$x_2 = \tfrac{1}{2} e^{t}(\xi_1 + \xi_2) - \tfrac{1}{2} e^{-t}(\xi_1 - \xi_2) \tag{25}$$

SUBOPTIMAL FEEDBACK CONTROL

We shall show the step from the optimal steering to a sub-optimal feedback control for the damped oscillator. We have seen, that there are two types of optimal control, the singular control, leading to the origin and the bang-bang control in the outer region.
Yet the control u is constrained. There-by the limits of the (stable) singular trajectories can be defined. They are shaped by a circle with the radius R (Fig. 2) which is the recoverable region for the singular control:

$$u = (1+b)x_1 + a x_2 \qquad (26)$$

The switching curves for the bang-bang type control in the outer region are approximated by straight lines:

$$u = -u_0 \operatorname{sign}(x_2 + d x_1 + \ell_0 \operatorname{sign} x_1) \qquad (27)$$

In order to build up this feedback control we have used some digital logic (see Fig. 3). The solution is given in Fig. 4.

2.-ORDER SYSTEMS WITH TIME-VARYING COEFFICIENTS

The 2.-order system with time varying coefficients now is treated as a more common type. Here it is not efficient to compute switching curves backward in time, because they are not stationary. But another consideration can help us. As shown, we got approximately straight lines for the system with constant coefficients. The signifying values of these straight lines are functions of a and b. Having (e.g.) periodic functions a(t) and b(t) we are able to compute their signifying values as functions of time, i.e. we get time varying straight lines and it is possible to use the same feedback control.

EXTREMAL SINGULAR CONTROL

There also exist extremal singular trajectories, as in the case of constant coefficients. We obtain a saddle point in the origin. The singular control is of the form:

$$u = [1 + b(t)]\, x_1 + a(t)\, x_2 \qquad (28)$$

So the area of admissible control is time-varying. The recoverable region has a variable radius R(t).

SUBOPTIMAL FEEDBACK CONTROL OF THE PITCHING MOTION OF A SATELLITE

The pitching motion of a satellite on an elliptic orbit is represented by the following equations:

$$A(\ddot{\vartheta} + \ddot{\tau}) = -3\Gamma m_E / R^3 (B - C)\vartheta \qquad (29)$$

$$R = \frac{p}{1 + e\cos\tau}\,; \quad \dot{\tau} = \Omega(1 + e\cos)^2\,; \quad \Omega = \sqrt{\Gamma m_E / p^3}$$

A B C	main inertial moments
Γ	gravity constant
m_E	mass of the earth
ϑ	pitch angle
τ	true anomalie
R	radius of the orbit
P	parameter of the orbit
e	excentricity

With $\vartheta' = d\vartheta/d\tau = \dot{\vartheta} \cdot 1/\dot{\tau}$ we obtain:

$$\vartheta'' - \frac{2e\sin\tau}{1 + e\cos\tau}\,\vartheta' + \frac{3}{1 + e\cos\tau}\,\frac{B - C}{A}\sin\vartheta\cos\vartheta = \frac{2e\sin\tau}{1 + e\cos\tau} \qquad (30)$$

The satellite moves on an elliptic orbit around the earth. ϑ being zero, one axis of the satellite directs to the centre of the earth. This position is to be controlled by an active feedback control.

With $\sin\vartheta \approx \vartheta$; $\cos\vartheta \approx 1$ our system has the form:

$$\begin{bmatrix} \vartheta_1' \\ \vartheta_2' \end{bmatrix} = \begin{bmatrix} 0 & 1 \\ -b(\tau) & -a(\tau) \end{bmatrix} \begin{bmatrix} \vartheta_1 \\ \vartheta_2 \end{bmatrix} + \begin{bmatrix} 0 \\ 1 \end{bmatrix} u + \begin{bmatrix} 0 \\ \frac{2e\sin\tau}{1 + e\cos\tau} \end{bmatrix} \qquad (31)$$

$$b(\tau) = \frac{3}{1 + e\cos\tau}\,\frac{B - C}{A}\,; \quad a(\tau) = -\frac{2e\sin\tau}{1 + e\cos\tau}$$

$a(\tau)$ and $b(\tau)$ given for $0 < \tau < 2\pi$ we know the switching lines of a corresponding system with constant coefficients. Fig: 7 shows the analogue program. The functions $d(\tau)$, $C_0(\tau)$ and $R^2(\tau)$ are generated by DFG's.

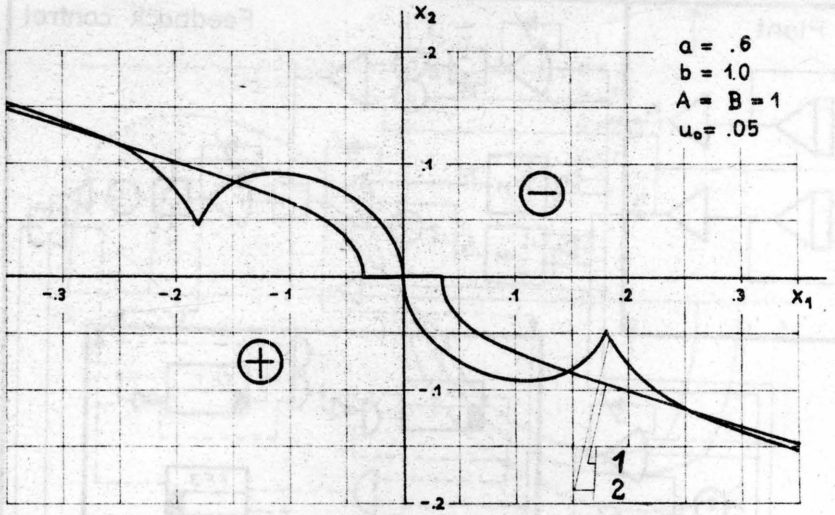

Fig.1: Switching curves for the 2.-Order Plant.

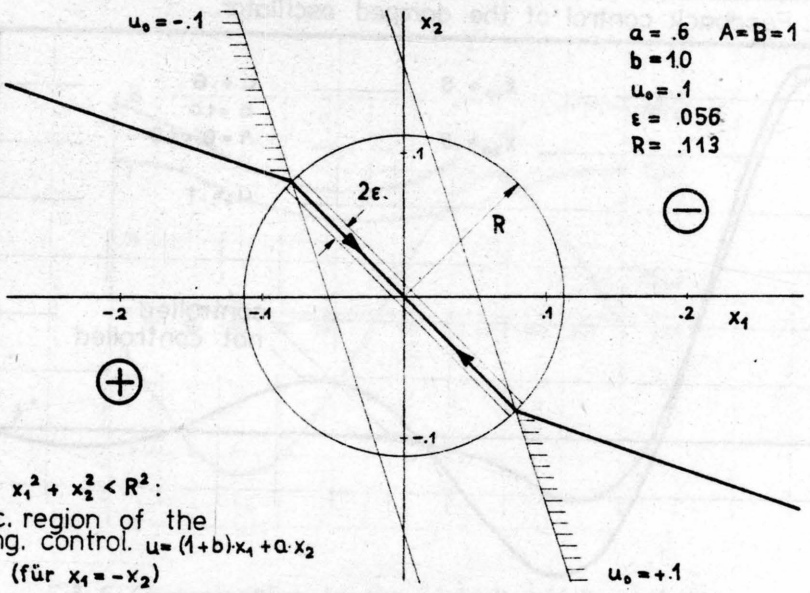

$x_1^2 + x_2^2 < R^2$:
rec. region of the
sing. control. $u = (1+b)x_1 + a \cdot x_2$
(für $x_1 = -x_2$)

Fig. 2: Switching curves for the feedback control of the damped oscillator.

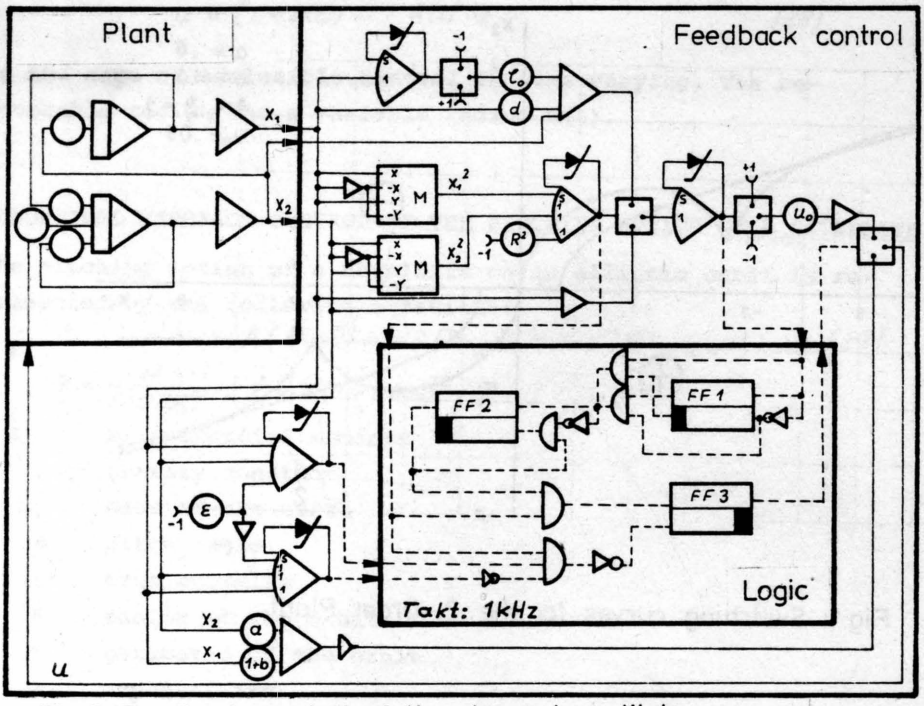

Fig.3: Feedback control of the damped oscillator.

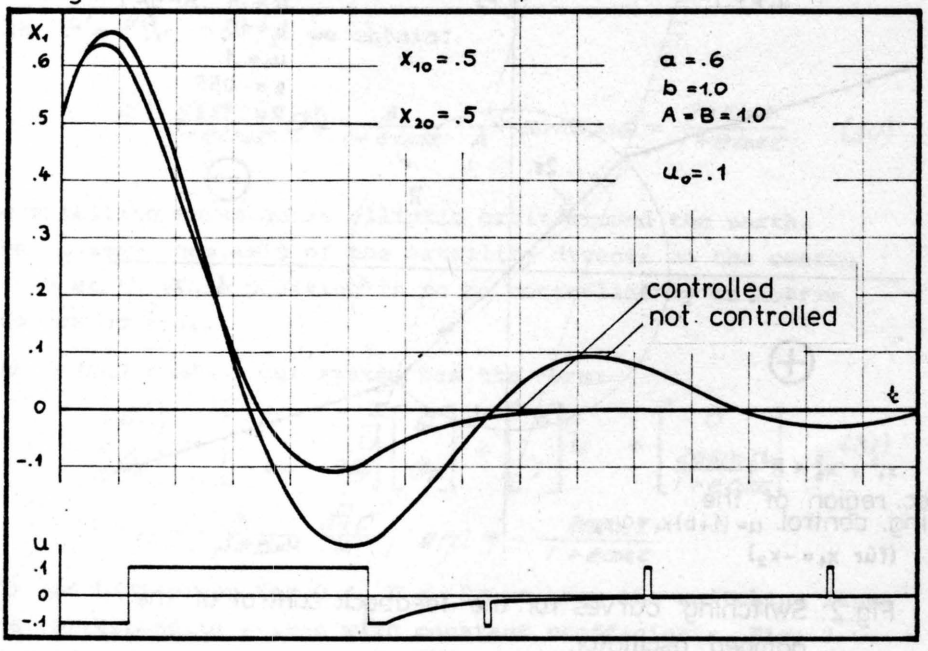

Fig.4: Output of the controlled and not controlled system.

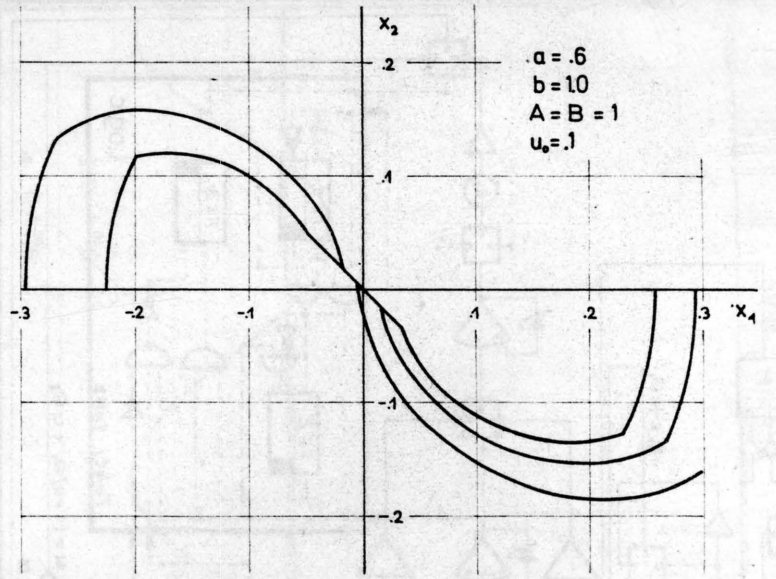

Fig.5: Phase plane trajectories for the contr. damped oscillator.

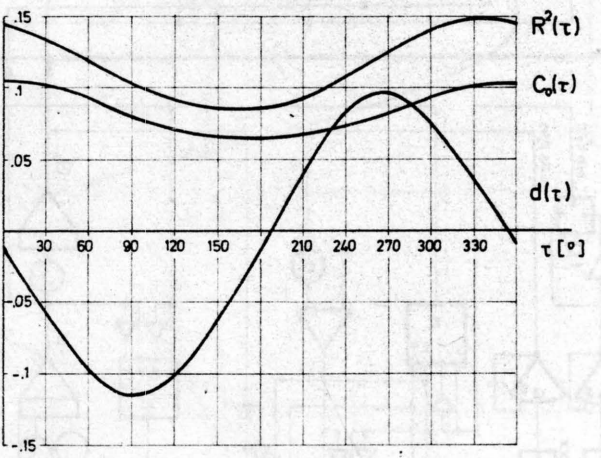

Fig: 6: Characteristics for the controller of the satellite.

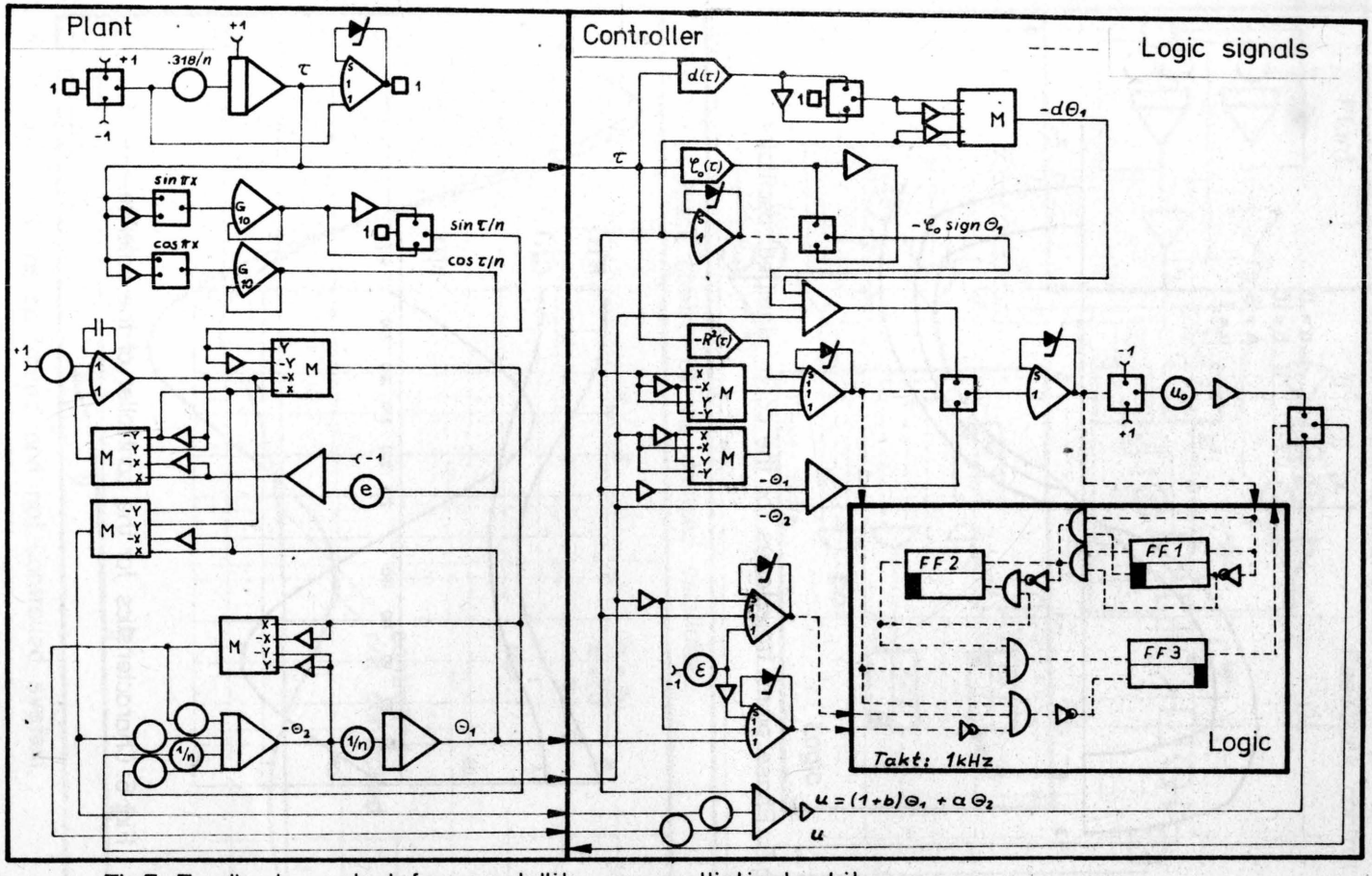

Fig.7: Feedback control for a satellite on an elliptical orbit.

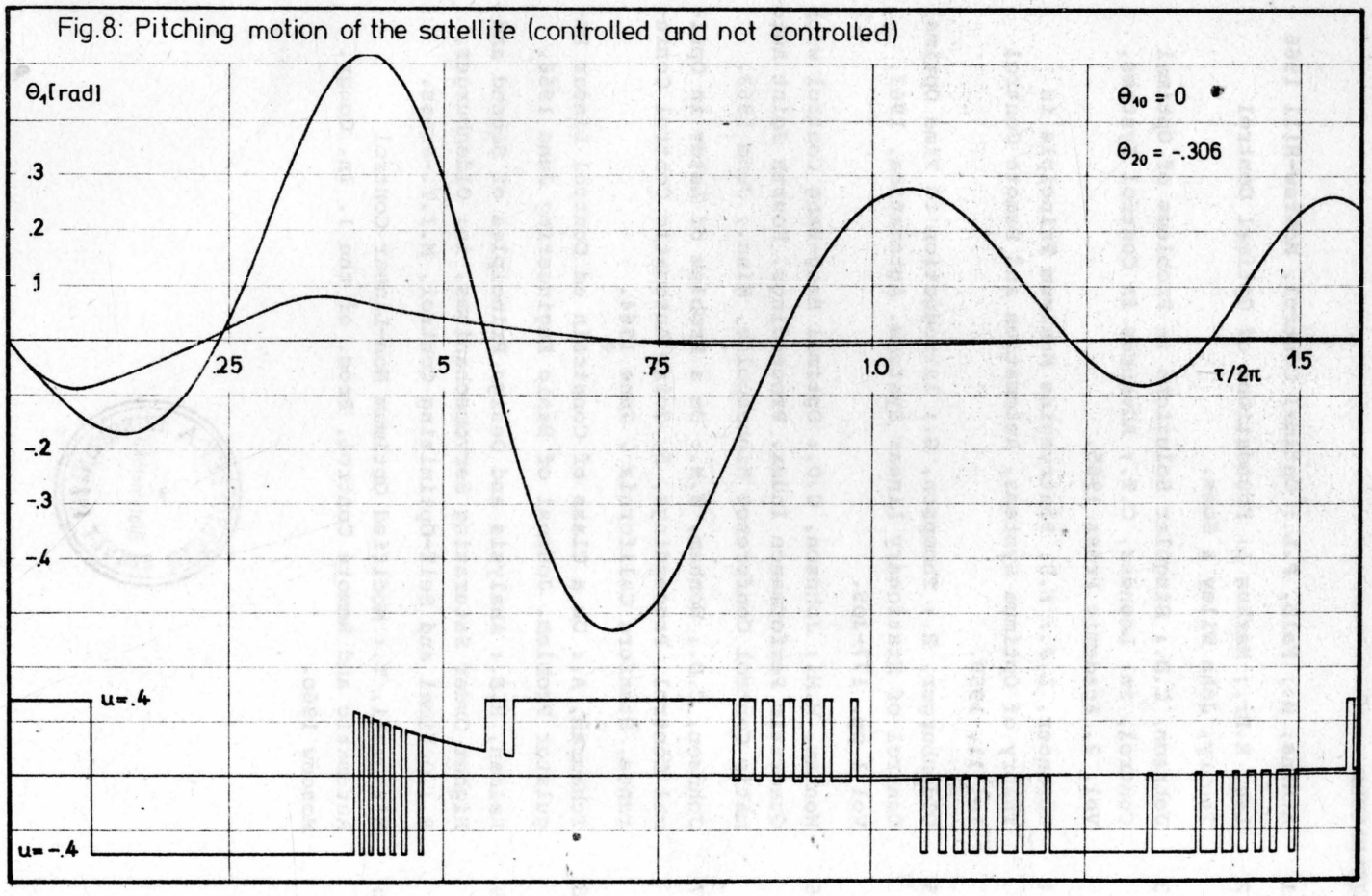
Fig.8: Pitching motion of the satellite (controlled and not controlled)
Θ_1[rad]
$\Theta_{10} = 0$
$\Theta_{20} = -.306$
.3
.2
.1
-.2
-.3
-.4
.25
.5
.75
1.0
1.5
$\tau/2\pi$
u=.4
u=-.4

LITERATURE

1 Athans, M.; Falb, P.L.: Optimal Control, McGraw-Hill 1966

2 Lee, E.Br.; Markus L: Foundations of Optimal Control Theory, John Wiley & Sons.

3 Johnson, C.D.: Singular Solutions in Problems of Optimal Control, in: Leondes, C.T.; Advances in Control Systems, Vol. 2, Academic Press 1965.

4 Rozonoer, L.J.: L.S. Pontryagins Maximum Principle in Theory of Optimum Systems, Automation and Remote Control 1o, 11, 1959.

5 Oldenburger, R.; Thompson, G.: Introduction to Time Optimal Control of Stationary Linear Systems. Automatica, 1963, Vol 1 pp. 177-2o5.

6 Wonham, W.M.; Johnson, C.D.: Optimal Bang-Bang Control with Quadratic Performance Index. Proceedings, Fourth Joint Automatic Control Conference Minneapolis, Minn., June 1963.

7 Johnson, C.D.; Wonham, W.M.: On a Problem of Letov in Optimal Control. Proceedings, 5. Joint Automatic Control Conference, Stanford California ; June 1964.

8 Tchamran, A.: On a Class of Constrain ed Control Linear Regulator Problem. Journal of Basic Engineering June 1966.

9 Kalman, R.E.: Analysis and Design Principles of Second and Higher Order Saturating Servomechanisms, in: Oldenburger, R.; Optimal and Self-Optimizing Control, M.I.T.-Press.

1o Mitsumaki, T.: Modified Optimum Non-Linear Control Automatic and Remote Control, Proc. of the 1. In. Congr. Moscow 196o.